ISOTOPIC GASEOUS SELF-DIFFUSION COEFFICIENTS AT TRANSITIONAL PRESSURES

by 149

GLEN ROY CORRELL

B. S., University of Missouri at Rolla, 1965

A MASTER's THESIS

submitted in partial fulfillment of the

requirements for the degree

MASTER OF SCIENCE

Department of Nuclear Engineering

KANSAS STATE UNIVERSITY
Manhattan, Kansas

1967

Approved by:

John O. Mingle

Major Professor

TABLE OF CONTENTS

1.0 INTRODUCTION AND THE THEORY OF GASEOUS DIFFUSION..... 1

1.1 Types of Gaseous Diffusion..... 1

1.2 Ordinary Gaseous Diffusion..... 2

1.3 Knudsen Diffusion..... 7

1.4 Transition Range Diffusion.....11

2.0 EXPERIMENTAL THEORY.....17

2.1 Introduction.....17

2.2 Methods for Measuring Diffusion Coefficients.....18

2.3 Analysis.....28

2.4 Semiconductor Radiation Detectors.....35

2.5.0 Experimental Facilities.....39

2.5.1 Diffusion Cell and Auxiliary Apparatus....39

2.5.2 Electronic Counting System.....46

2.6.0 Reduction of Data.....48

2.6.1 Preparation of Data for Analysis.....48

2.6.2 Standard Deviation Analysis.....52

3.0 RESULTS AND DISCUSSION.....56

3.1 General Discussion.....56

3.2 Conclusion.....64

4.0 SUGGESTIONS FOR FURTHER STUDY.....65

5.0 ACKNOWLEDGEMENT.....67

6.0 LITERATURE CITED.....68

7.0 APPENDICES.....75

7.1 APPENDIX A: Solution to the Differential Equation for Diffusion through a Capillary Tube.....76

TABLE OF CONTENTS (continued)

7.2 APPENDIX B: Leakage Error Analysis.....83

7.3 APPENDIX C: Data Analysis for the Diffusion Coefficient.....87

7.3.1 Computer Program.....87

7.3.2 Least Squares Analysis and Numerical Approximations.....87

7.4 APPENDIX D: Experimental Procedures.....90

7.5 APPENDIX E: Error Associated with Pressure Gradients.....95

LIST OF TABLES

I. Sample set of count-rates versus time data taken from the analyzer output.....50

II. Experimental and theoretical results for the self-diffusion coefficient of carbon dioxide in the transition pressure range.....57

III. Experimental and theoretical results for the self-diffusion coefficient of methane in the transition pressure range.....59

LIST OF FIGURES

1. Effective self-diffusion coefficients for CO_2 and CH_4 at 20°C with a 0.1026 cm I.D. tube.....16

2. Simplified experimental diffusion cell assembly with system parameters.....29

3. Transient response curve for CO_2 with a 0.1026 cm I.D. and 10 cm length capillary tube.....33

4. Transient response curve for CH_4 with a 0.1026 cm I.D. and 10 cm length capillary tube.....34

5. Schematic diagram of diffusion cell and auxiliary apparatus for CH_4.....40

6. Assembly of diffusion cell apparatus (electrical and light shields not shown).....41

7. Surface-barrier radiation detector before insertion into operating position.....42

8. Block diagram of complete counting system.....43

9. Comparison between experimental and theoretical self-diffusion coefficients for CO_2.....58

10. Comparison between experimental and theoretical self-diffusion coefficients for CH_4.....60

NOMENCLATURE

A_n	Coefficient of the $n^{\underline{th}}$ term of the summation, defined with Eq. (B-10)
C	Concentration of tagged material at z
C_o	Concentration of tagged material in flask I at zero time
C_1	Concentration of tagged material in flask II and capillary tube at zero time
C_∞	Concentration of tagged material in system at equilibrium
c	Number of constraints
D	General diffusion coefficient, cm^2/sec
D'	Approximate diffusion coefficient defined in Eq. (B-7), cm^2/sec
D_{Bi}	Diffusion coefficient of species i at atmospheric pressure, cm^2/sec
$D_{e_{ij}}$	Effective diffusion coefficient (refers to diffusion in transition range) of species i in species j, cm^2/sec
D_{Ki}	Knudsen diffusion coefficient of species i, cm^2/sec
D_{ij}	Diffusion coefficient of species i in species j according to bulk diffusion theory, cm^2/sec
F	Pressure-induced flow term, $g\text{-moles}/cm^2\text{-sec}$
f_D	First two terms of Taylor's series expansion for the partial of Re with respect to D
$f_i(\underline{r},\underline{v_i},t)$	Distribution function
$\vec{J}$	Mean molecular flow, $molecules/cm^2\text{-sec}$
K_n	Knudsen number, ℓ/r
k	Boltzmann constant for a molecule
k_i	Proportionality constant

L	Effective length of capillary tube, cm
L'	Half-length of capillary tube, cm
$L[f(t)]$	Laplace transform of f(t)
$L^{-1}[f(s)]$	Inverse Laplace transform of f(s)
ℓ	Mean free path length, cm
M_i	Molecular weight of species i, gm/g-mole
m_i	Molecular mass of species i, gm
N_i^*	Molecular transport of species i in molecules per unit time
$(N-c)$	Number of degrees of freedom associated with σ_X^2
n_i	Number of molecules of species i per unit volume
P	Pressure
R	Gas constant per gram
Re	Residue
r	Radius of capillary tube, cm
s	Laplacian variable
T	Absolute temperature, °K
T_{ij}^*	Temperature dependent potential energy parameter for i-j interaction, (ε_{ij}/k)
$T_{1/2}$	Half-life of pressure gradient decay, sec
t	Time
V_1	Volume of tagged reservoir, cm^3
V_2	Volume of untagged reservoir, cm^3
$\bar{v}$	Arithmetic mean speed, cm/sec
$X(\xi,\tau)$	Dimensionless concentration variable, (C/C_o)
Xc_i	Calculated value of X at time i
Xe_i	Experimental value of X at time i

X_{ia}	Approximated value of X at time i
X_{∞}	Equilibrium value of X
Y_{1a}, Y_{1b}	Mole fractions of species 1 at each end of the diffusion path
z	Distance variable along tube
α	Dimensionless parameter for volume of tagged reservoir, (R^2L/V_1)
α'	Defined with Eq. (20)
β	Dimensionless parameter for volume of untagged reservoir, (R^2L/V_2)
ΔD_L	Correction of the diffusion coefficient for finite tube length, cm^2/sec
ΔX_d	Change in the normalized activity in flask I by diffusive flow
ΔX_T	Total change in the normalized activity in flask I
ΔX_F	Change in the normalized activity in flask I by pressure-induced flow
γ	Euler's constant
ε_{ij}	Force constant for i-j interaction
λ_n	Eigenvalues of transcendental equation
μ	Gas viscosity, poise
ξ	Dimensionless distance variable, (z/L)
ρ	Density
σ	Molecular diameter
σ_D	Standard deviation for D
$\sigma_D^2(N)$	Variance for D obtained by least squares analysis
$\sigma_D^2(P)$	Variance for D caused by uncertainties in pressure measurements
σ_i	Molecular diameter of species i

σ_P^2	Variance of pressure measurements
σ_X	Standard deviation of least squares calculation of $X(\xi,\tau)$
σ_X^2	Variance of $X(\xi,\tau)$ calculation by least squares analysis
σ_{ij}	Effective diameter of 1-2 interaction
τ	Dimensionless time variable, (tD/L^2)
Θ_n, Φ_n	Coefficient variables defined with Eq. (A-22)
$\psi_{n_i m_i}$	Net flux of species i, gm/sec-cm^2
Ω_{ij}	Potential energy parameter for i-j interaction

1.0 INTRODUCTION AND THE THEORY OF GASEOUS DIFFUSION

1.1 Types of Gaseous Diffusion

A vast amount of scientific interest and effort has been and continues to be focused on transport phenomena--the transport of momentum, energy, and mass within matter--for their common and almost universal occurrence necessitates an understanding of them to ensure the success of myriad undertakings in basic and applied science and engineering. While the phenomena are quite analagous in many respects, their differences are sufficient to warrant and require their individual study.

The similarities of the phenomena are demonstrated by the conventional definitions of the transport coefficients. The coefficients of viscosity, thermal conductivity, and diffusion are defined as the negative ratios of the net fluxes of momentum, energy, or mass to the gradients of these. The definition of the diffusion coefficient in a macroscopic system in one dimension in equation form is

$$\psi_{n_i m_i} = -D \frac{dn_i m_i}{dz} \tag{1}$$

where $\psi_{n_i m_i}$ = the net flux of species i, gm/sec-cm^2

D = the diffusion coefficient, cm^2/sec

$n_i m_i$ = the concentration of species i, gm/cm^3

n_i = the number density of species i, molecules/cm^3

m_i = the mass of a molecule of species i, gm/molecule

z = the distance variable along which diffusion occurs

The particular topic of this study is gaseous diffusion in the transition pressure range, one of the three broad subdivisions of gaseous diffusion. The other subdivisions are: (1) Ordinary, or bulk diffusion; and (2) Knudsen diffusion. A brief discussion of each subdivision follows with an outline of the kinetic theory of gases whose concepts are common to all three.

1.2 Ordinary Gaseous Diffusion

In any real gas, the molecules travel in all directions with a wide distribution of velocities, and molecular interactions are quite complex because of long range attractions and short range repulsions. However, a surprisingly useful, although oversimplified, model for the behavior of a gas containing n molecules per unit volume may be formulated based on the following assumption:

1) The molecules are rigid, non-attracting spheres with diameter σ.
2) All the molecules travel with the same speed; a reasonable choice is the arithmetic mean speed; for a Maxwellian speed distribution, $\bar{v} = (8kT)^{1/2}(\pi m)^{-1/2}$ cm/sec.
3) All the molecules travel in a direction parallel to one of the coordinate axes.

Because of the first assumption, collisions between molecules are well defined, and a quantity known as the mean free path, the average distance traversed by a molecule between collisions, may be introduced. By use of the other assumptions and the ideal gas law ($p=nkT$), this quantity may be shown (36) to be

$$\ell = kT/k_1 P\pi\sigma^2 \quad , \quad \text{cm} \tag{2}$$

$$\text{where } k_1 = (1/3) + (2/3)\sqrt{2} \quad .$$

(If the speed distribution were assumed Maxwellian with molecular motion in all directions, the result would be the same except that k_1 would be equal to $\sqrt{2}$). For simple molecules σ is about $3\text{x}10^{-8}$ cm and at one atmosphere pressure and 20 degrees C. the mean free path of a gas molecule is approximately given by $\ell = 10^{-5}/p$ cm where p is in atmospheres. It can be shown (36) that by the simplified kinetic theory the diffusion coefficient is given by

$$D_{11} = \bar{v}\ \ell/3 = k_2(\pi mkT)^{1/2}(\pi\sigma^2\rho)^{-1} \quad , \text{ cm}^2/\text{sec} \tag{3}$$

where $k_2 = 2/(3\pi)$

$\rho = Pm/kT$, the density of the gas.

Although the mean free path does not appear directly in a rigorous development, the solution is of the same form. However, a rigorous derivation shows that k_2 should be $3/(8\pi)$. By inserting this value and combining constants, the expression becomes

$$D_{11} = 2.628 \times 10^{-3}\ T^{3/2}(M^{1/2}P\sigma^2)^{-1} \quad , \text{ cm}^2/\text{sec} \tag{4}$$

It should be noted that this expression is for self-diffusion, the inter-diffusion of particles of the same mass and size. Using the same rigid sphere model the diffusion coefficient for a mixture of two species, D_{12}, according to Hirschfelder (36) is

$$D_{12} = 2.628 \times 10^{-3} \, T^{3/2}(M_1+M_2)^{1/2}(2M_1M_2)^{-1/2}(P\sigma_{12})^{-1} \ , \ cm^2/sec \quad (5)$$

where $\sigma_{12} = (\sigma_1+\sigma_2)/2$, cm

As would be expected, although the rigid sphere model yields reasonable results, these results give only approximate pressure and temperature dependence of the diffusion coefficient because of the severe restrictions entailed by the simplicity of the model. Rigorous kinetic theory allows prediction of these dependencies with considerably greater accuracy by considering the effects of interactions which take place between real molecules. For most purposes it is most convenient to describe these interactions by use of potential energy functions which describe the potential energy of interaction. Two of these functions which are commonly used (36) are the Lennard-Jones potential for non-polar molecules and the Stockmayer potential for polar molecules. While these two functions are idealizations of the true energy of interaction, many of the properties of gases (and liquids) have been calculated in terms of them, and they are reasonably adequate for a number of simple molecules.

The rigorous development of the kinetic theory of gases is based on a knowledge of the distribution function, $f_i(\underline{r},\underline{v}_i,t)$, which represents the number of molecules of i^{th} species which at time t lie in a unit volume element about the point $\underline{r}$ and which have velocities within a unit range about $\underline{v}_i$. Under equilibrium conditions, $f_i(\underline{r},\underline{v}_i, t)$ reduces to the Maxwellian velocity distribution (36). When the system is not at equilibrium, the

distribution functions satisfies the Boltzmann integro-differential equation.

For the usual definition of the diffusion coefficient to apply, i.e., for the derivatives of the flux vectors to be linear a gaseous system must be near equilibrium. In this limit the distribution function is nearly Maxwellian, and the Boltzmann equation can be solved by perturbation methods of Chapman and Enskog (12). Expressions for mass flux and the diffusion coefficient may be obtained from this solution.

These expressions show that mass transfer may be produced not only by a concentration gradient, but also by a temperature gradient. This fact is not displayed in the derivation by the simple kinetic theory.

Neglecting temperature effects, the first approximation to the diffusion coefficient for a binary mixture by the Chapman-Enskog theory is

$$D_{12} = 2.628 \times 10^{-3}\, T^{3/2} (M_1+M_2)^{1/2} (M_1 M_2)^{-1} (P \sigma_{12}^2 \Omega_{12} T_{12}^*)^{-1} \ , \ cm^2/sec \qquad (6)$$

where D_{12} = diffusion coefficient in cm^2/sec,

P = pressure in atmospheres,

T = temperature in degrees K,

$T_{12}^* = kT/\varepsilon_{12}$,

$M_1 M_2$ = molecular weights of species 1 and 2, respectively, gm

σ_{12}, ε_{12}/k = molecular potential energy parameters characteristic of 1-2

interaction in Å and degrees K, respectively,

Ω_{12} = a complicated potential energy parameter which indicates the deviation of any particular molecular model from the idealized rigid-sphere model.

When the above equation is written for a single component, the coefficient of self-diffusion is given by

$$D_{11} = 2.628 \times 10^{-3} \, T^{3/2} (M^{1/2} p \sigma_{11}^2 \Omega_{11} T^*_{11})^{-1} \text{ , } cm^2/sec \qquad (7)$$

where D_{11} = coefficient of self-diffusion in cm^2/sec, and the other parameters are the same as before.

It should be noted that here the diffusion coefficient is proportional to $T^{3/2}$ and inversely proportional to the pressure as it was in the expression derived from simple kinetic theory. However, these proportionalities are now modified by the presence of Ω and T^* which adjust the coefficient for molecular interactions.

The Chapman-Enskog theory of gases has generally been adopted and is considered sufficient for this study for use in the investigation of gaseous systems under limited conditions. The causes of these limitations are assumptions in this treatment which restrict the applicability of the results. Since only binary collisions of molecules are considered, the theory is not applicable at elevated pressures where the frequency of collisions of three or more molecules at once becomes appreciable. Because of the

use of classical mechanics in the derivations, the theory is inapplicable at low temperatures where relativistic phenomena become significant considerations. The Chapman-Enskog method for solution of the Boltzmann equation provides a series approximation to the distribution function. The first approximation, which defines the diffusion coefficient conventionally in terms of the first derivative of the concentration is applicable only when this gradient is small. Higher approximations provide corrections for larger gradients, but thus redefine the diffusion coefficient. Quantitatively, the first approximation is valid only when the relative changes in the concentrations in the distance of a mean free path are small compared with unity. A further assumption in development of the theory is that the dimensions of the containing vessel are large compared to the mean free path, a condition which is not met by rarefied gases in moderately small containers. Since this study is concerned primarily with rarefied gases, these two last restrictions necessitate the investigation of other models for the treatment of low pressure phenomena. Finally, the Chapman-Enskog theory of gases applies only to monatomic gases, strictly speaking; however the diffusion process is not appreciably different for polyatomic molecules, provided the deviation from a spherical shape is small.

1.3 Knudsen Diffusion

As the pressure of a gaseous system is decreased, the frequency of collisions of molecules with each other decreases and

the mean free path of the molecules, ℓ, increases. The probability of a molecule reaching a wall of the containment vessel thus increases and the effects of intermolecular collisions eventually become negligible when compared with those of molecule-wall collisions. This situation occurs when the Knudsen number, K_n, which equals ℓ/r for a tube of radius r, is greater than 10. Under this condition, there is little mechanism for the establishment of local equilibrium and free-molecule or Knudsen flow occurs. This flow is analogous to a process of diffusion and occurs for each constituent along the gradient of its partial pressure or its concentration gradient.

If the pressure of the system is indeed low enough to make the effects of intermolecular collisions negligible, the characteristics of this flow may be determined by consideration of molecule-wall interactions only. Knudsen (47) experimentally determined that the reflection of gas molecules from a glass wall is almost 100% diffuse and follows the cosine reflection law. He assumed that this was caused by irregular roughness of the surface on the atomic scale. However, the work of Langmuir (48,49) and Volmer and Estermann (76) demonstrated that gas molecules are not reflected by a simple impact and rebound mechanism. Rather, gas molecules are absorbed on impact and after a finite time are evaporated. Thus every surface, no matter how smooth, will in theory reflect gas molecules according to a cosine law.

If the actual irregular container wall surface is replaced by a smooth mathematical surface and if it is assumed that the adsorbed film is in equilibrium with the gaseous phase, the

number of molecules desorbed may be obtained by proceeding as if the desorbed molecules originated in an equilibrium gas layer on the other side of the surface. The number of molecules desorbed from a unit area of the wall per unit time in a particular direction is then equal to the number crossing the unit area of the mathematical surface in that direction. This quantity is obtained by integrating over all the speeds of the molecules within some solid angle about the direction of interest. Using this expression for the distribution of the molecules moving in a particular direction, the net transport through a cross section of the container can be calculated. For a long tube, Present (60) shows that this quantity is

$$N^* = - (2\pi r^3 \bar{v}/3) \, dn/dz \tag{8}$$

or converting to mean flow per unit area per unit time

$$\bar{J} = - (2\bar{v} \, r/3) \, dn/dz \quad . \tag{9}$$

Equation (9) shows that Knudsen flow has the characteristics of diffusion--it is proportional to the negative concentration gradient--and the diffusion coefficient is seen to be

$$D_K = 2 \, \bar{v} \, r/3 \ , \ cm^2/sec \quad . \tag{10}$$

This is quite similar to the bulk diffusion coefficient, $(\bar{v} \, \ell/3)$, and as would be expected the mean free path length, ℓ, has been replaced by the diameter of the confining tube.

It is noted that in Knudsen flow, the diffusion coefficient D_K is proportional to $T^{1/2}$, to the pore diameter, and is independent of the total pressure. Using an assumed Maxwellian velocity distribution the result becomes

$$D_K = (2r/3)(8kT/\pi m)^{1/2}$$

$$= 9700\, r(T/M)^{1/2} \text{ cm}^2/\text{sec} \quad , \qquad (11)$$

Where D_K = coefficient of Knudsen diffusion in cm^2/sec,

r = pore radius in cm,

M = molecular weight of the species, gm

T = absolute temperature in ^oK.

For a pore diameter of 1.026mm at 20^oC and at a pressure for which $K_n = 10$, D_K equals 1284 cm^2/sec for carbon dioxide and 2127 cm^2/sec for methane. For the diffusion of CO_2 in N_2 at 25^oC in a pore of radius 0.05 cm, D_K and D_{11} become the same at a pressure of 89.2 microns. For diffusion at one atmosphere pressure the coefficients are equal for a pore size of 588 Å.

If Knudsen flow of a binary gas mixture occurs, the component gases will diffuse along the tube independently and Eq. (8) can be applied to each gas separately if n is assumed to refer to one species of molecules in the mixture. For steady flow, n must be constant along the tube; therefore, the density gradient $\frac{dn}{dz}$ is uniform and can be replaced by $\Delta n/L$ where Δn is the difference in density between the ends and L is the tube length. Since $\Delta n = \Delta p/kT$ from Eq. (8), the flow rate in moles is

$$F(\text{moles}) = (D_K \pi r^2)\,\Delta P/LRT \quad , \text{moles/sec} \tag{12}$$

where F applies to the component with partial pressure drop Δp, and R is the gas constant per gram. It is noted that the flux of a particular component is inversely proportional to its molecular weight. These formulae for Knudsen flow have a sound theoretical basis and have been verified by experimental work.

1.4 Transition Range Diffusion

As has been discussed, the mechanism of Knudsen gaseous diffusion is well understood and rigorously explained as is Poiseuille or bulk diffusion. The important range of transition from Knudsen to bulk diffusion encompasses a thousandfold range of mean free paths. Typical chemical process conditions fall in this transition range when common pelleted catalysts with a pore diameter of a few millimicrons are utilized. Increased interest in ballistics problems arising from flight in the upper atmosphere has accentuated the need for further investigation of this intermediate region. The small pore diameter of the catalyst pellets produces a large value for the Knudsen number, as do the long mean free path lengths of the upper atomsphere. In either case, Knudsen effects and transitional behavior result.

The net transport through a cross section of a long tube under conditions of Knudsen flow is given by Eq. (8). Pollard and Present (59) state that in the high pressure limiting form at uniform total pressure the analagous expression for self diffusion is

$$N_1^* = (\pi r^2 D_{11}/kT)\; dP_1/dz. \tag{13}$$

In the absence of a total pressure gradient and the associated molecular drift velocity, the diffusive transports which may occur are amenable to kinetic theory treatment so that it should be possible to discuss theoretically the transition from Eq. (8) to Eq. (13). Pollard and Present show that for a tube of infinite length considering both bulk and Knudsen self-diffusion

$$N_1^* = -(\pi r^2 \bar{v} \ell/3)[1-3\ell/(8r) + (6\ell/(\pi r))Q(r/\ell)]dn_1/dz \qquad (14)$$

where

$$Q(r/\ell) = \int_0^{\pi/2} \cos\theta d\theta \int_0^{\pi/2} e^{-2r\cos\theta\csc\psi/\ell} \cos^2\psi \sin^2\psi d\psi \ . \qquad (15)$$

Although the evaluation of $Q(r/\ell)$ often requires numerical techniques, an expression which can be used for small values of r/ℓ is

$$Q(r/\ell) = \pi/16 - \pi r/(6\ell) + \pi r^2/(3\ell^2)$$

$$- (\pi/3)[1.2264 - (3/4)\ln(2\gamma r/\ell)] \ r^3/\ell^3 + \ldots \qquad (16)$$

where γ is Euler's constant.

From Eq. (14) the diffusion coefficient is given as

$$D_{e_{11}} = (\bar{v}\ \ell/3)\ [1-3\ell/(8r) + (6\ell/(\pi r))Q(r/\ell)] \ . \qquad (17)$$

Pollard and Present further state that for a finite tube of half length L' the diffusion coefficient must be reduced from that for an infinite tube by a factor

$$\Delta D'_L = (\bar{v}\, r/2)\left[e^{-L'/\ell} + (L'/\ell)\mathrm{Ei}(-L'/\ell)\right](r/L') \quad . \tag{18}$$

This correction term is negligible for mean free paths a few times shorter than the half length of the tube.

Eq. (17) agrees very closely with an earlier expression advanced by Bosanquet (6)

$$D_{e_{11}}^{-1} = D_{K_1}^{-1} + D_{11}^{-1} \tag{19}$$

which states that the resistance to transport is the sum of resistance caused by wall collisions and intermolecular collisions. It is derived by considering the diffusion process in the tube as a random walk process in which the successive steps of the individual molecules are terminated either by collisions with other molecules or with the tube wall. The mean step size is then related to the mean free paths for wall collisions and gas collisions by taking the total collision frequency to be $\bar{v}/\ell$. The additive resistance law results then from knowledge that the frequencies of the two types of collisions are additive and that D_K and D_{11} can be taken proportional to $\bar{v}$ times the mean step size. This relationship is probably the most widely accepted for the diffusion coefficient in the transition pressure range.

Scott and Dullien (67) support Bosanquet's expression through a derivation based on the Stefan-Maxwell momentum balance method (60) in a binary system. A momentum balance on the molecules of species 1 is made in a differential volume element by equating the net flux of momentum carried in and out of the volume element.

From this balance an expression for the net molecular transport of 1 is derived

$$N_1^* = (P/RTL)(D_{12}/\alpha')\ln\{(1-\alpha' y_{1b} + D_{12}/D_{K1}) \cdot (1-\alpha' y_{1a} + D_{12}/D_{K1})^{-1}\} \tag{20}$$

where $\alpha' = 1 + N_2^*/N_1^*$,

y_{1a} and y_{1b} refer to the mole fraction of 1 at the ends of the diffusion path.

By equating N_1^* as derived from momentum with N_1^* as given by a usual simple diffusion coefficient

$$N_1^* = D_{e_{12}} P/RTL(y_{1a}-y_{1b}) \tag{21}$$

the effective diffusion coefficient is shown to be

$$D_{e_{12}} = D_{12}/x_{LM} \tag{22}$$

where X_{LM} is the logarithmic mean average of X_1 and X_2,

$$X_{LM} = (X_2-X_1)\ln X_1/X_2 = \alpha'(y_{1a}-y_{1b})\ln\{(1-\alpha' y_{1a}+D_{12}/D_{K1}) \cdot (1-\alpha' y_{1b} + D_{12}/D_{K1})\} \quad . \tag{23}$$

The definitions of X_1 and X_2 are

$$X_1 = 1 - \alpha' y_{1a} + D_{12}/D_{K1} \quad ,$$

and

$$X_2 = 1 - \alpha' y_{1b} + D_{12}/D_{K1} \quad .$$

For self diffusion, α' is zero, and the expression of $D_{e_{11}}$ reduces to that of Bosanquet.

Rothfeld (66) presents a derivation similar to that of Scott and Dullien. Evans, Watson, and Mason, (22) also support Bosanquet's relation by a rather unusual treatment. Theirs is a model in which a porous solid diffusion medium (such as a catalyst pellet) is visualized as a collection of spherical particles which are very large in size as compared to a gas molecule. The system is then treated as a "dusty" gas in which the dust particles are held stationary. By formally treating the dust particles as giant "molecules" which are merely one component of a multicomponent mixture, the problem becomes one of classical kinetic theory of multicomponent mixtures.

Wheeler (82) proposes an exponential function to define D_e

$$D_{e_{11}} = D_{11}(1 - e^{-D_{11}/D_{K1}}) \quad . \tag{24}$$

However, his reasoning is primarily intuitive and the relationship admittedly semi-empirical. This is the only expression found in the literature which deviates significantly from Bosanquet's relationship. For CO_2 and CH_4 systems at 20°C this effective diffusion coefficient is shown in Fig. 1 as a function of pressure for diffusion through a 1.026 mm I.D. tube. It is noted that these combinations rules disagree in the range of three to three hundred microns of mercury. This, in essence, comprises the transition range.

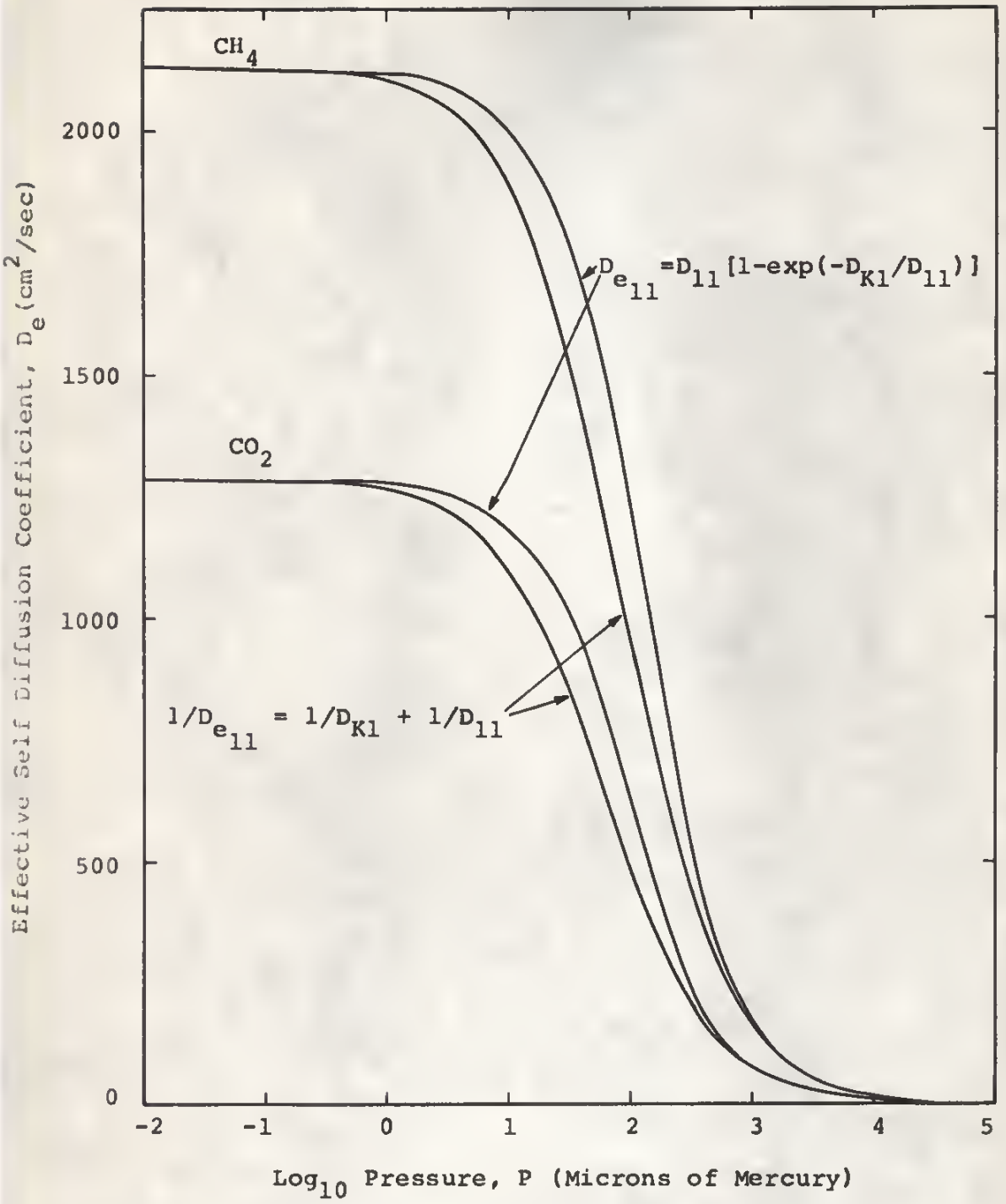

Figure 1. Theoretical effective self diffusion coefficients for CO_2 and CH_4 at 20°C with a 0.1026 cm I.D. tube (from Eqs. (7, 11, 19, and 24)).

2.0 EXPERIMENTAL THEORY

2.1 Introduction

The experimental arrangements used to measure gaseous diffusion coefficients all have in common the establishment of a concentration gradient for the component of interest. These arrangements, however, are quite distinct in other respects as are the methods of analysis applied to them. The experimental arrangements can be generally classified in two groups: (I) steady-state type experiments in which flow streams of different compositions pass on opposite sides of a barrier through which diffusion occurs, or (II) transient experiments in which diffusion eliminates an initial concentration difference between two parts of a closed batch system. The methods of analysis may similarly be divided as: (A) those based on Fick's first law equation, or (B) those based on his second law equation. Systems which yield themselves to method (A) generally have the advantage of much simpler mathematical descriptions, but frequently are more demanding in experimental equipment and technique. Type (I) experiments are illustrative of this point; they have the advantage of straightforward analysis based on Fick's first law equation, but require large amounts of material and precise flow control. Early measurements by method (I) were made by Buckingham (10) on porous soil; more recent measurements on catalysts and absorbents include those of Scott and Dullien (67), Otani and co-workers

(56), Evans and co-workers (22), and Wakao and Smith (77). Type (II) experiments regardless of the method of analysis require measurements of concentrations as functions of time, and these measurements have been their primary source of difficulty. The development of radioactive tracer techniques and particularly the development of semiconductor radiation detectors has lessened the difficulty of making internal measurements of concentration without disturbing the system.

The lack of attention to the determination of diffusion coefficients in the transition pressure range has been notable in the past. Only recently have attempts been made to measure gaseous mutual and self-diffusion coefficients under conditions of mixed Knudsen and bulk diffusive flow. The apparatus used in this experiment was designed to measure diffusive flow through a capillary tube under these conditions by the use of radioactive tracers and a semiconductor radiation detector. While other investigators have utilized radioactive tracer techniques it is believed that Mistler's (53) is the only other work using a semiconductor detector. The following survey of earlier techniques serves to illustrate the advantages of this method.

2.2 Methods of Measuring Diffusion Coefficients

Most of the measurements of the gaseous mutual-diffusion coefficient have been based on a method attributed to Loschmidt (51). In its simplest form, the apparatus consists of a long, closed, vertical tube that can be divided into two equal sections by a

removable partition at its center. The upper half is filled with the lighter gas and the lower half with the heavier gas, both at the same temperature and pressure. The partition is removed and the two gases are allowed to diffuse into each other for a measured amount of time.

Concentration measurements may be in the form of a detection device, generally at one end of the tube, or the total amount of the diffusing material in one of the cylinders may be determined by suitable means. Either method requires solution of the partial differential equation produced by application of Fick's second law equation. (Jost (44) and Crank (15) give rather complete summaries of the mathematical description of the various geometrical diffusion assemblies requiring analysis by method (B) with various initial concentration distributions). In the case of concentration measurements by use of a detector, the Fourier power series solution of the concentration, in terms of the diffusion coefficient, tube length, and time, may be used to evaluate the diffusion coefficient. In this latter case, the data, consisting of the time for diffusion and the composition of the gas mixtures contained in both portions of the cylinder, are put into proper forms of the integrated Fourier power series and the diffusion coefficient is evaluated. Tordai (74) has presented an analysis of the Loschmidt method showing the possibility of accuracies to within 0.3%. Strehlow (71) has reported values with less than 2% error by use of a modified Loschmidt cell.

An interferometric method of measuring mutual diffusion coefficients based on the Loschmidt geometry was presented by Boyd,

Stein, Steingrimsson, and Rumpel (7) in 1951. In this method the change in composition of the gas at a fixed position in the diffusion cell is determined by measuring the change in refractive index with an interferometer. Several determinations of the binary diffusion coefficient, D_{12}, can be made during the course of a run, and values accurate to within 0.5% have been obtained by this method.

Boardman and Wild (4) simulated the conditions for self-diffusion by using gases with molecules of equal mass in a Loschmidt cell. Using mixtures of nitrous oxide and carbon dioxide, D_{11} for either gas was found to be 0.0107 cm^2/sec at 15°C and one atmosphere pressure. By the method of Kelvin triads, (45) they also determined D_{11} for hydrogen, nitrogen, and again for carbon dioxide. In this method, D_{12} is determined for each of the three pairs of gases found in a ternary system and σ_{12} is calculated. Since $\sigma_{12} = (1/2)(\sigma_{11} + \sigma_{22})$, values for each of the three σ_{12}'s allow solution for each value of σ_{11}.

The Loschmidt method and related methods are quite time consuming, and it is very difficult to estimate the effect of concentration on diffusivity. Coward (14) gives an indication of the time required for Loschmidt type determinations. He indicated that each run is allowed to go on for sixty minutes and then the mixtures are allowed to stand overnight before being analyzed. Boardman (4) indicates minimum diffusion time of one hour and a maximum of six hours.

The method of Loschmidt is quite inconvenient and difficult to use in evaluating the diffusion coefficient of liquid vapors into gases. Stefan (70) devised a method which makes such evaluations relatively simple and convenient for reasonably volatile liquids. A sample of the liquid, whose vapor diffusion coefficient is to be measured, is placed in the bottom of a vertical tube. With the tube maintained at constant temperature, the second component, a gas, is passed over the top of the tube at a rate sufficient to keep the partial pressure of the vapor there at a value essentially corresponding to the initial composition of the gas, i.e., zero in the case of a vapor-free gas. The diffusion of the vapor out of the tube affects a slow lowering of liquid level. The rate of evaporation of the liquid is simply related to the diffusion coefficient. As with the Loschmidt method, the data, consisting of the time of gas flow and the amount of liquid evaporated, are put into proper integrated forms of the diffusion equations and D_{12} evaluated.

In 1957 Walker and Westenberg (78) introduced a significant new flow method for measuring the diffusion coefficient of gases called "the point source technique". This shortened significantly the time period required for an experiment. The method made use of the steady injection of a trace gas from a fine hypodermic tube into a slow, laminar, uniform stream of a second carrier gas. Measurements were made by thermal conductivity cells on the concentration of the trace gas in both the radial and longitudinal directions. The diffusion coefficient could be calculated from

either the radial or longitudinal data with an error of approximately 1%. By heating the carrier gas the measurements may be extended to fairly high temperatures. Also the trace gas concentrations involved are essentially zero, so that uncertainties regarding the concentration dependence of the diffusion coefficient are avoided. The method has been used to study $He-N_2$, N_2-CO_2, He-A, and CO_2-He-N_2 (78, 79, 80, 81).

Ember, Ferron, and Wohl (20) have modified the point source technique to permit investigation at higher temperatures through the use of a thin, flat flame which burns at the base of the apparatus. They also used radioactive tracer techniques enabling them to measure self-diffusion coefficients.

Bohemen and Purnell (5) and Giddings and Seager (27, 28, 29) first successfully demonstrated that diffusion coefficients at low pressures could be measured accurately by the use of gas chromatographic techniques. The apparatus used consisted of a gas chromatography unit with an empty tube replacing the packed column. Reported binary coefficients agreed with published results within 1%. Giddings et al (30) and Evans and Kennedy (21) have extended this technique over a range of temperatures and pressures. Knox and McLaren (46) modified the method to another method called "arrested elution method" for measurement of diffusion coefficients at low pressures. They reported $D_{12} = 0.165$ cm^2/sec for ethylene in nitrogen at 18°C and 750 mm which was in agreement with the literature value.

Knudsen (47), Gaede (26), and Adzumi (1) were the first to investigate the flow of gases in the transition pressure range. Knudsen's apparatus consisted of two flasks of approximately 1000 ml volume each, joined by a capillary tube with a mercury cutoff valve. He found that a minimum specific flow occurred at a pressure corresponding to approximately $r/\ell = 0.3$. Gaede repeated his measurements with an arrangement which used a rectangular slit in place of the capillary tube. He verified Knudsen's findings but erroneously attributed the minimum to an absorbed layer of molecules which restricted flow. Adzumi also verified Knudsen's results with similar equipment and used several tubes of different bores at both low and intermediate pressures.

The closest approximation to self-diffusion is accomplished by use of isotopic molecules. The intermolecular forces and effective cross sections for interactions between isotopic molecules are essentially the same as for interactions between identical molecules of the isotopic pair. The only noticeable difference between the isotopic diffusion coefficient and the idealized self-diffusion coefficient results from the change in the reduced mass which is $M_1/2$ or $M_2/2$ for self-diffusion. The first isotopic diffusion measurements were made by Harteck and Schmidt (33) for the interdiffusion of the ortho and para forms of hydrogen using a Loschmidt cell. This method was later used by Groth and Harteck to determine the coefficients of krypton and xenon (32). A more accurate method of making isotopic-diffusion measurements was developed in 1943 by Ney and Armistead (54). Since

nearly all subsequent measurements of self-diffusion have utilized the Ney-Armistead technique, and since it is most similar to that used in this study, it will be described in some detail.

The Ney-Armistead apparatus differs from that of Loschmidt in that two large chambers are used with a straight tube or pipe connecting them. In the original apparatus the connecting tube consisted of two equal-sized copper pipes with a section of neoprene tubing between them; by pinching the rubber with a clamp, the two-chambers could be isolated. One chamber was filled with a sample enriched in $U^{235}F_6$ and the other with a sample enriched in $U^{238}F_6$. With both chambers at the same pressure and temperature, the diffusion process was started by unpinching the neoprene. Samples from one chamber were slowly bled through an adjustable capillary leak into the ion source of a mass spectrometer in order to follow the concentration changes. Diffusion coefficients were reported to within 4%. This method has two advantages over the Loschmidt technique: (1) the geometry is more compact, reducing the errors associated with thermal gradient; and (2) continuous concentration measurements allow several determinations of the diffusion coefficient within one experiment.

The theory of the Ney-Armistead method is based on four assumptions: (1) that the diffusion coefficient is independent of concentration; (2) that the composition of the gas in the chambers is uniform, the concentration gradient being confined to the connecting tube; (3) that the concentration in the connecting tube varies linearly with distance along the tube; and (4) that

the volume of the connecting tube is negligible compared with the volume of the chambers. Assumption (1) is justified for self-diffusion but not for mutual diffusion; according to kinetic theory the mutual diffusion coefficient is independent of concentration only to a first approximation. A discussion of the validity of the other assumptions has been presented by Paul (58). The second assumption is justified providing a small end correction is made. Actually, the concentration gradient extends slightly beyond the ends of the tube, and the correction is made by replacing the measured length of the tube by a slightly greater effective length. Analysis of the analogous electrical case by Maxwell (52) and Rayleigh (63) shows that the length of the tube should be replaced by an effective length 1.642r greater. Assumption (3) is found to be valid after the decay of initial transients. This decay requires only a few seconds, a negligible time in the original experiments. Finally, a small correction proportional to the ratio of the volume of the capillary tube to that of the chambers may be made in order to account for the effect of the tube volume. Based on the above assumptions, Ney and Armistead applied Fick's first law to obtain an expression for the concentration of an isotope in the chamber being analyzed as a function of time. Knowledge of the physical parameters allowed a solution for a diffusion coefficient.

Hutchinson (39) determined the self-diffusion coefficient of argon over a range of temperatures by observing the diffusion of A^{41} with a modified Ney-Armistead apparatus. He showed that

the self-diffusion coefficient of a gas can be obtained from the coefficient of diffusion of one isotope into another by the following relationship:

$$D_{11} = [2m_2/(m_1+m_2)]^{1/2} D_{12} \qquad (25)$$

where m_1 and m_2 refer to the molecular masses of the isotopes. The concentrations of A^{41} in both chambers were measured by the ion currents drawn to insulated electrodes inserted into each chamber. Winn investigated the $N^{14}N^{14}$--$N^{14}N^{15}$ system (84) and the temperature dependence of the self-diffusion coefficients of A, Ne, N_2, O_2, CO_2, and CH_4 (85) using the Ney-Armistead apparatus. Winn and Ney (83) used the same method for investigation of CH_4 self-diffusion for pressures ranging from 515 mm to 630 mm and temperatures ranging from 19.2°C to 24.7°C.

The radioactive tracer, $C^{14}O_2$ has been frequently used to measure diffusion coefficients. Admur (2) measured diffusion coefficients within 2% for CO_2-CO_2, CO_2-N_2O,Xe-Xe, and A-Xe systems using a Loschmidt device. The ionization currents from electrodes in the cells were used to measure concentration changes. Drickamer (40,73) utilized a scintillation detector in a modified Loschmidt cell to measure diffusion coefficients of CO_2-CO_2 and CO_2-CH_4 systems over a pressure range from 0.5 to several atmospheres. Diffusion coefficients for CO_2 were determined by O'Hern and Martin (55) from 0° to 100°C and at pressures to 200 atm. They used a modified Ney-Armistead apparatus. Winter (86,87) used a Nev-Armistead arrangement to measure diffusion coefficients of CO_2, O_2, and N_2. Visner (75) has made the only study of gas

diffusion in the transition pressure range using a diffusion tube with well defined dimensions, i.e., an empty capillary tube instead of a chamber packed with porous material. He used a modified Ney-Armistead cell with end-window Geiger counters installed in both flasks to follow concentration changes. The self-diffusion coefficient of xenon was measured for capillaries of 0.0025 cm and 0.025 cm radius in tubes of three lengths for pressures corresponding to radius to mean free path ratios from 0.001 to 65. The trace gas was injected into one flask after filling the flasks to the desired pressure with normal gas by breaking a tiny glass bulb of gas at the correct pressure to prevent the creation of a pressure gradient across the capillary tube.

An apparatus called a diffusion bridge was used by Bendt (3) to measure the diffusion coefficient for He^3-He^4 and H_2-D_2 at one atmosphere pressure and temperatures from 1.74°K to 296°K. The measurement was made while steady-state flow existed through four capillaries and through the diffusion tube which joined the supply and exhaust capillaries in the temperature bath. The pressure gradient in the diffusion tube was made as small as possible by adjusting the flow rates of the gases through the capillary feed lines. The exhaust capillaries were alternately connected to a mass spectrometer for gas analysis. Small fluctuations in the flow rates and in the sensitivity of the mass spectrometer limited the accuracy of the measurements to an error of 2-6%. The correction factors used were the Rayleigh tube length correction and the mass correction formula (Eq. 25) for isotopic self-diffusion measurements.

In contrast to the numerous reports of use of $C^{14}O_2$ as a tracer in diffusion measurements, no mention of a similar use of $C^{14}H_4$ was found in the literature. Winn (85) and Winn and Ney (83) used $C^{13}H_4$-$C^{12}H_4$ for isotopic diffusion measurements of CH_4, but the stability of C^{13} precluded the use of tracer techniques and they relied upon mass spectrography for concentration measurements. It appears quite possible that the use of $C^{14}H_4$ as a tracer in determination of self-diffusion coefficients for CH_4 is a unique feature of this study.

The above survey has included a discussion of all common techniques used to measure diffusion coefficients. The Ney-Armistead method has been emphasized because it allows a simple and accurate means of studying gas diffusion in the transition pressure range. Additional surveys of recent experimental and theoretical work on the diffusion of gases have been made by Liley (50) and Johnson (41,42,43). A discussion of information on diffusivity needed by the chemical and process industries has been presented by Friend and Adler (25).

2.3 Analysis

The diffusion cell used in this study was of the Ney-Armistead type and is depicted in Fig. 2. To make a measurement of the effective diffusion coefficient, both flasks were evacuated and then filled with gas at the same temperature and pressure. The gas in flask I included a trace of radioactive gas. (See Appendix C for a detailed description of experimental procedure).

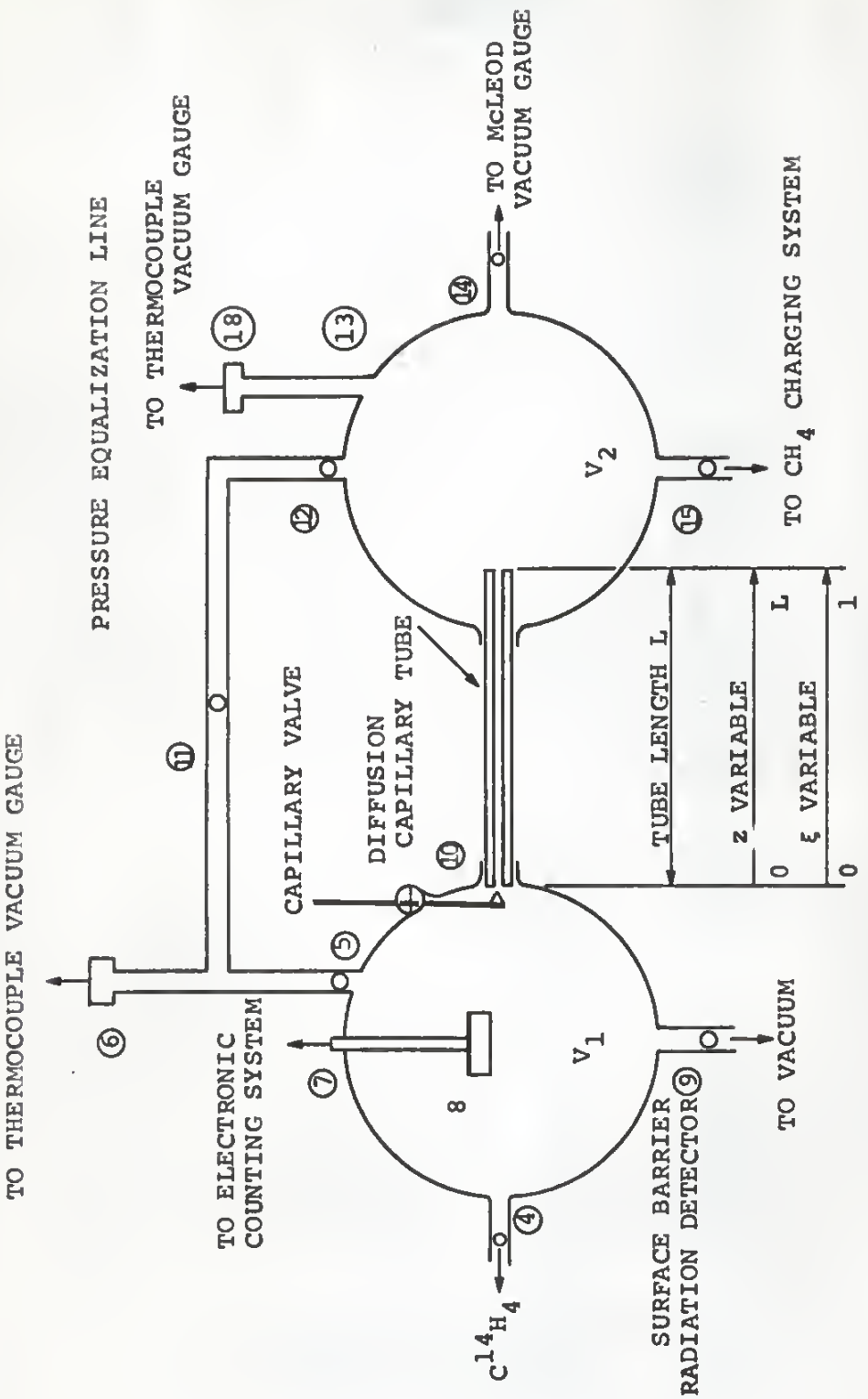

Figure 2. Simplified experimental diffusion cell assembly with system parameters (for CH_4).

Following the opening of the capillary tube valve a one dimensional diffusion process was established in which the molecules of radioactive gas from flask I intermixed with the gas from flask II until the system was of constant composition throughout its volume. The amount of material transferred by self-diffusion was then directly proportional to the change in radioactivity in flask I. This change in activity as a function of time was measured by use of a semiconductor radiation detector.

Description of the diffusion process in the tube by Fick's second law caused only Ney and Armistead's first and second assumption to be required. Based upon these assumptions and the use of Fick's second law the resulting partial differential equation for diffusion through the tube was

$$\frac{\partial C}{\partial t} = D \frac{\partial^2 C}{\partial z^2} \tag{26}$$

where C = the concentration of radioactive gas at time t at position z, D = the diffusion coefficient, and z = the distance along the tube length.

The boundary conditions for Eq. (26) were:

$$t = 0,\ z > 0,\ C = C_1 \tag{27}$$

$$t > 0,\ z = 0,\ C\big|_{z=0} = C_o - V_1^{-1} \int_0^t (-D\pi R^2) \frac{\partial C}{\partial z}\bigg|_{z=0} dt \tag{28}$$

$$t > 0,\ z = L,\ C\big|_{z=L} = C_1 + V_2^{-1}\left(\int_0^t (-D\pi R^2)\frac{\partial C}{\partial z}\Big|_{z=0}\, dt - \right.$$

$$\left.\int_0^L \pi R^2 C\, dz + C_1 \pi R^2 L\right) = C_1 + V_2^{-1} \int_0^t (-D\pi R^2)\frac{\partial C}{\partial z}\Big|_{z=L} dt \qquad (29)$$

where V_1 = volume of flask I (tagged)

V_2 = volume of flask II (untagged)

L = effective tube length

R = radius of tube

C_o = initial concentration of radioactive gas in flask I

C_1 = initial concentration of radioactive gas in flask II and tube

C = concentration of radioactive gas as a function of t and z.

Equation (27) states that at time zero the concentration of tagged material in the tube and flask II is C_1. Equation (28) shows that the amount of radioactive gas in flask I is the original amount less that leaving the flask by diffusion into the capillary tube. The final boundary condition, Eq. (29) states that the amount of tracer material in flask II is the original amount plus that entering from the tube; the amount entering from the tube may be evaluated directly as in Eq. 29 or as the total of that leaving the flask I and that originally in the tube less the amount remaining in the tube. This latter form is shown in Eq. (29).

The complete solution to Eq. (26) is

$$X(\tau,\xi) = (\beta+\alpha x_1[\beta+1])(\alpha+\beta+\alpha\beta)^{-1} + (X_1-1)\sum_{n=1}^{\infty}[\exp(-\lambda_n^2\tau)]$$

$$\cdot[\lambda_n\cos\lambda_n+\beta\sin\lambda_n][\alpha\cos(\lambda_n\xi) - \lambda_n\sin(\lambda_n\xi)]$$

$$\cdot\{\lambda_n^2[(2\lambda_n)^{-1}(\alpha+\beta+\alpha\beta-\lambda_n^2)\cos\lambda_n - \sin\lambda_n$$

$$\cdot(1+(\alpha+\beta)_2)\}^{-1} \quad . \tag{30}$$

where λ_n are the non zero roots of

$$\tan\lambda_n = \lambda_n(\alpha+\beta)(\lambda_n^2-\alpha\beta)^{-1} \quad . \tag{31}$$

A detailed solution of Eq. (31) by the method of Laplace transforms is given in Appendix A as well as a description of the dimensionless variables employed.

The time response of the system used is shown in Figs. (3) and (4) where the concentration of tracer in flask I is shown as a function of time for selected pressures. Figure (3) is for self-diffusion in a CO_2 system while Fig. (4) is for a CH_4 system. It should be noted that extremely accurate short time measurements are not required and that the rate of response may be easily varied by changing the tube length.

Equation (30) relates the concentration of the tagged gas to time at a position z inside the cell in terms of the diffusion coefficient, D, and the cell dimensions. An application of least squares analysis (33) to the concentration versus time data using

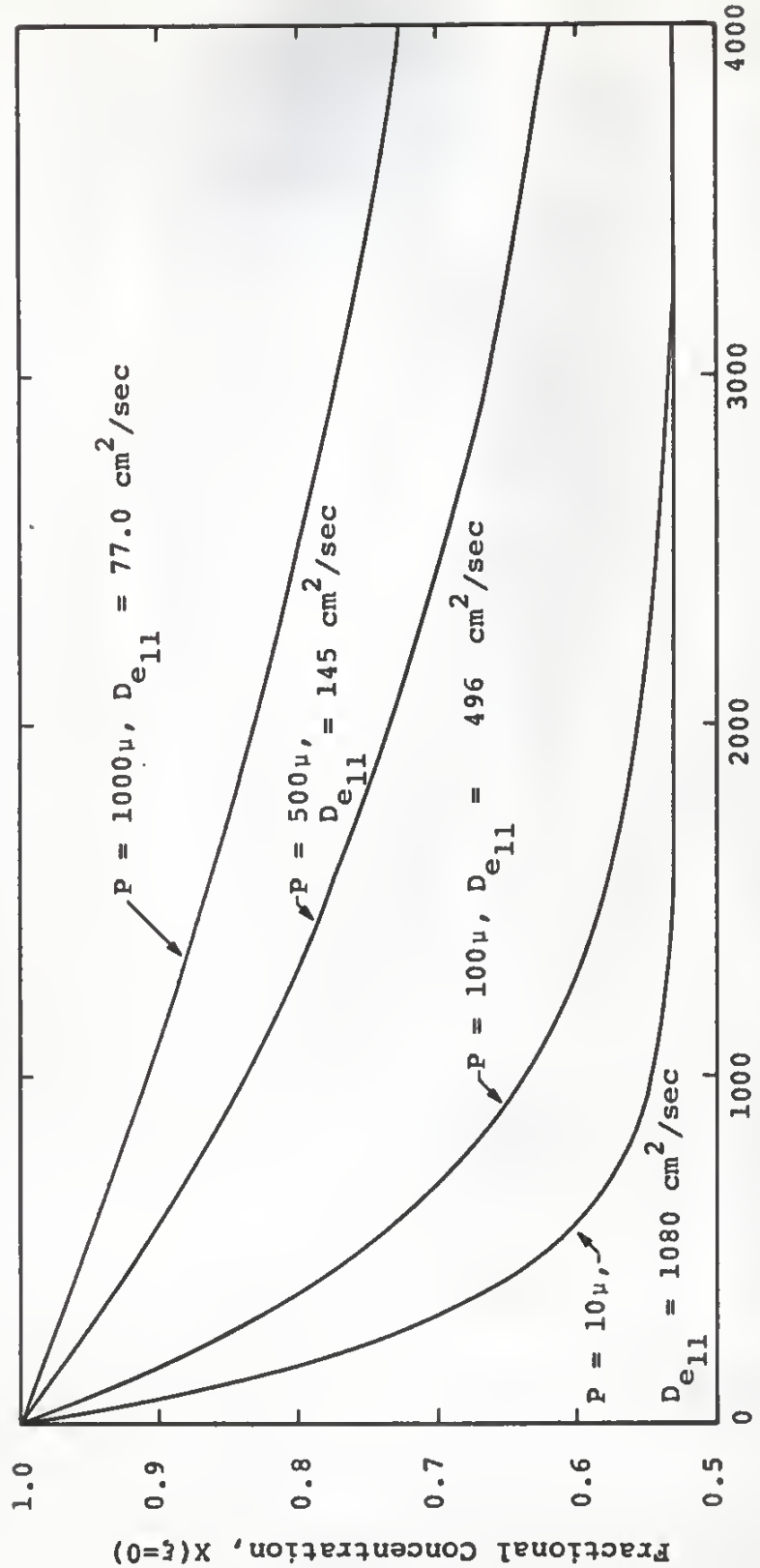

Figure 3. Transient response curve for CO_2 with a 0.1026 cm I.D. and 10 cm length capillary tube.

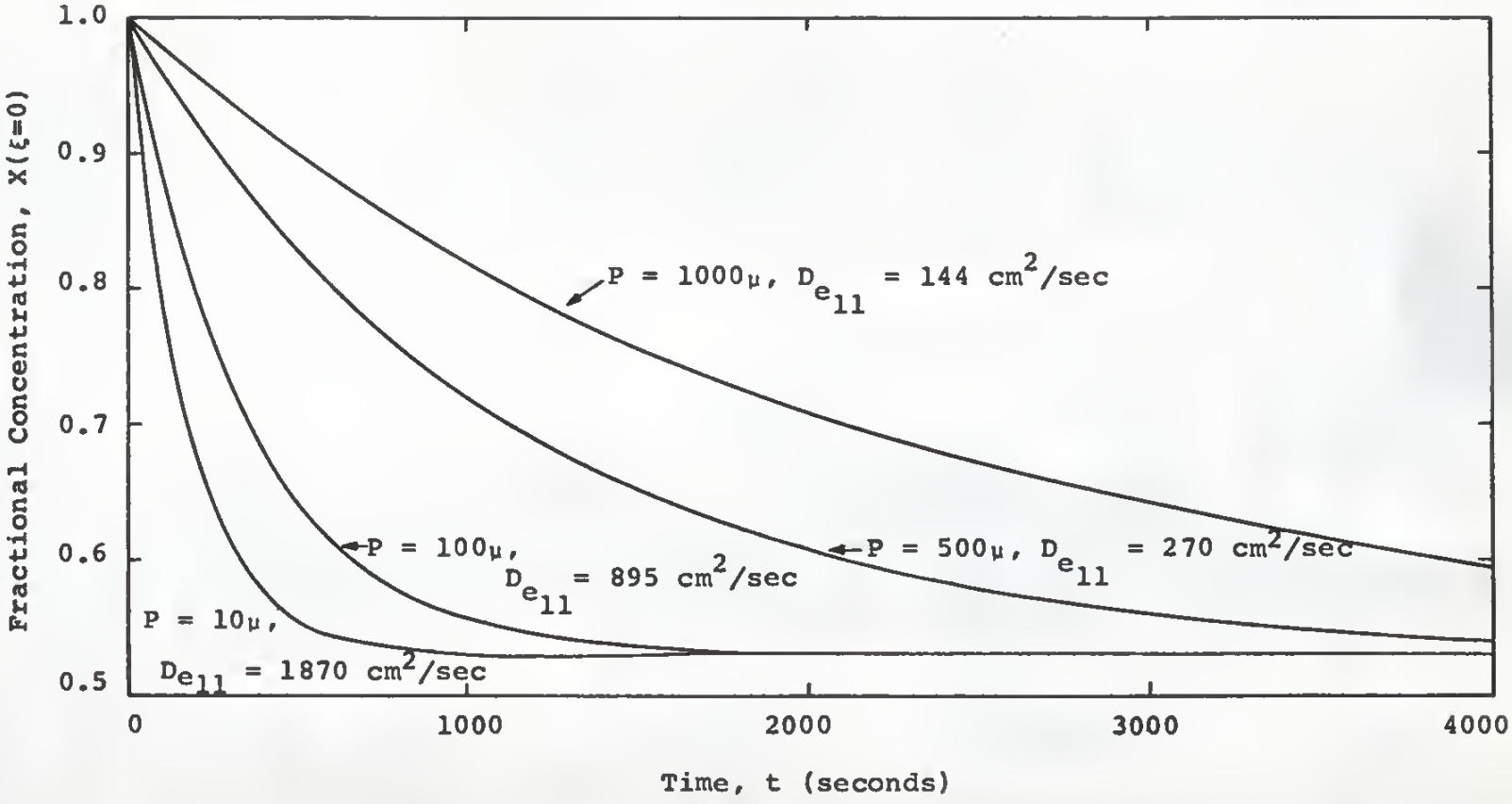

Figure 4. Transient response curve for CH_4 with a 0.1026 cm I.D. and 10 cm length capillary tube.

Eq. (30) and the appropriate system parameters yields an evaluation of the diffusion coefficient. A detailed discussion of the procedure for applying least squares analysis to the evaluation of D is given in Appendix C as well as an estimate of the error involved. In this experiment the tube length was determined by measuring and applying the Rayleigh end-correction used by Ney and Armistead. The other system parameters were measured as outlined in section 2.5.

Based upon the assumption of continuous mixing at the pressure of the measurement, which has been shown to be valid by Visner (74), the radioactivity measured by the surface-barrier detector was linearly proportional to the concentration of tracer in flask I. Because of the rapid response, the thin window, and the high counting efficiency of the detector it was not necessary to make dead time or other corrections on the activity data. The properties of semiconductor detectors are discussed in section 2.4.

2.4 Semiconductor Radiation Detectors

As a result of rapid technological advances in design and production techniques semiconductor radiation detectors have attained wide acceptance and usage in the last few years (8,16,17, 37,38,61). The demand for their development is readily explained by a brief review of their advantages. A semiconductor radiation detector approximates an ideal ionization chamber. This is accomplished by replacing the conventional gas of the ionization

chamber by solid semiconductor materials of high stopping power. The linear response of the signal pulse size (1 electron pair/3.5 ev) to the energy dissipated in the detector by an ionizing particle make semiconductor detectors particularly suitable for measurements of energy spectra. The high stopping power greatly reduces the probability of a particle traversing the active volume without complete dissipation of its energy. Semiconductor detectors have the further advantages of small size, low weight, thin window thickness, low operating voltage, precisely controlled sensitive depth and geometry, rapid time response, stability, and durability.

Semiconductor detectors utilize the properties of a junction of an n-type, donor-rich material with a p-type, acceptor-rich material (69,72). The application of a reverse electrical bias to the junction causes a migration of electrons in the n-type material toward the p-type material and holes in the p-type toward the n-type. The results of these movements are the establishment of a space charge region caused by an unbalanced concentration of filled electron acceptor sites and empty donor sites on opposite sides of the junction and the formation of a carrier free region of high resistance. This carrier free region is termed the depletion zone. Its depth is proportional to the square root of the product of the bias voltage and the dielectric resistivity. This depth generally ranges from 2 to 3 mm depending on the type of detector.

Goulding (31) presents a discussion of the applications and properties of the different types of semiconductor detectors.

The three commonly used types are: (1) the silicon-diffused junction type; (2) the lithium-drifted silicon or germanium type; and (3) the silicon surface-barrier type. The methods of preparation of these types in the same order are: (1) diffusion of n-type phosphorous into p-type (boron doped) silicon; (2) injection of n-type lithium ions deep into p-type silicon or germanium; and (3) evaporation of a thin layer of p-type gold on the surface of n-type silicon.

A silicon surface-barrier detector was used in this study. If an ionizing particle possesses sufficient energy to penetrate the thin gold film and a portion of the depletion region and impinges the surface at an angle which allows this, it will create electron pairs as it dissipates its energy in the sensitive volume. The electron pairs are separated by the space charge and attain a drift velocity as they migrate toward the electrical poles of the space charge. This motion induces a charge in the bias circuitry. By use of a charge sensitive preamplifier with negative capacitive feedback this charge may be converted to a voltage pulse which is essentially independent of detector capacitance.

The accuracy of measurements made with a surface-barrier detector is directly related to the ratio of the rate of true signal propagation to that of noise or spurious signals. Spurious signals may be generated within the amplification system or within the detector itself. Noise generation within the amplification system is best avoided by careful selection of the preamplifier and amplifiers. Discussions of these considerations are presented

by Fairstein (24) and Radeka (62). The primary sources of detector noise are microplasma breakdown, edge leakage currents, and charge carrier generation and recombination in the depleted volume. Detector noise may be minimized by selection of a high quality detector with a small, thin depletion region and operation at minimum temperatures. The detector should also have low electrical capacitance, but the capacitance is proportional to the ratio of the area of the depletion region to its thickness. Thus a compromise must be made in selecting the depletion thickness. The choice depends largely upon the intended use.

The use of a surface-barrier detector requires that several other requirements be met. All signal leads and the detector must be shielded to prevent the generation of noise resulting from electromagnetic radiations. The detector is also sensitive to visible light and must be in a thoroughly darkened enclosure. The signal lead from the detector to preamplifier should be of minimum length to reduce input capacitance. All electronic equipment should be connected to common grounds to avoid ground loop problems.

The detector bias voltage must be stable and well regulated. This voltage should be chosen so as to give the best signal to noise ratio. The speed and efficiency of charge collection within the detector increase monotonically with increasing voltage. The noise level also increases with detector bias following an initial decrease until a breakdown of the detector occurs. The noise level may be monitored as bias voltage is increased by use of an RMS voltmeter, an oscilloscope, or a multichannel analyzer.

Every precaution should be taken to avoid damaging the detector. The fragile gold surface-barrier must not be damaged by the application of sudden or combined stresses. The detector must be protected from chemical contamination, continued exposure to high radiation fluxes, and excess bias voltage.

2.5.0 Experimental Facilities

A diffusion cell apparatus and an electronic counting system comprised the experimental facilities used in making all measurements. With a radioactive component diffusing from one flask to a second flask joined by a capillary tube, the radioactivity in the charged flask provided a continuous measurement of the diffusion occurring through the opening in the capillary tube. The diffusion cell employed has similarities to those of earlier investigators, especially to those of Hutchinson (39), O'Hern and Martin (55), Winter (87), Ney and Armistead (54), and Timmerhaus and Drickamer (73). Figures 2, 5, 6 and 7 illustrate the diffusion cell and auxiliary apparatus. The electronic counting system, diagrammed in Fig. 8 consisted of a semiconductor radiation detector and a scaling circuit.

2.5.1 Diffusion Cell and Auxiliary Apparatus

A top view of the Pyrex glass diffusion cell mounted in the unfilled water bath is shown in Fig. 6. Referring to Fig. 5, flask I represents the side of the system charged with radioactive carbon dioxide and containing the surface-barrier semiconductor

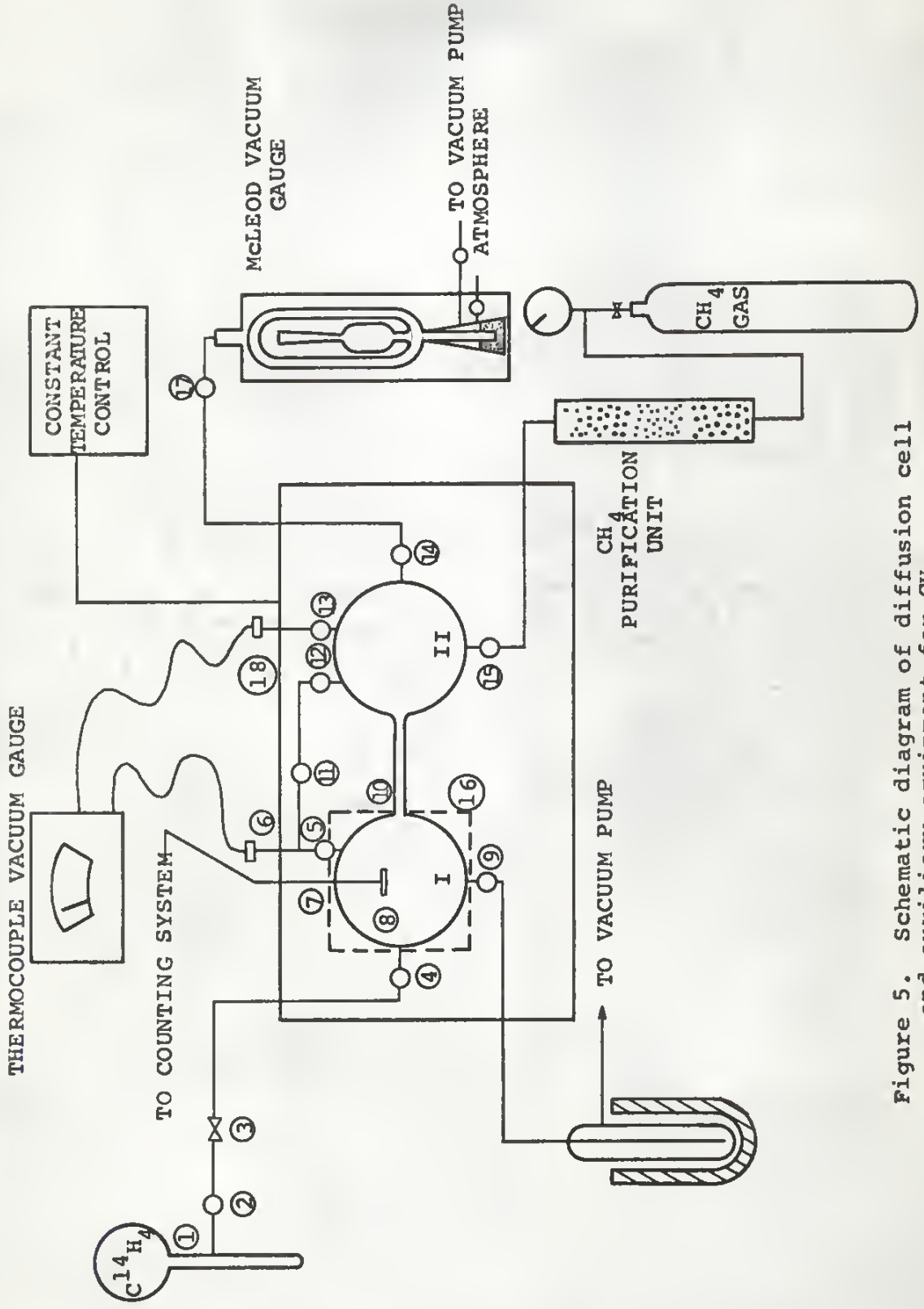

Figure 5. Schematic diagram of diffusion cell and auxiliary equipment for CH_4.

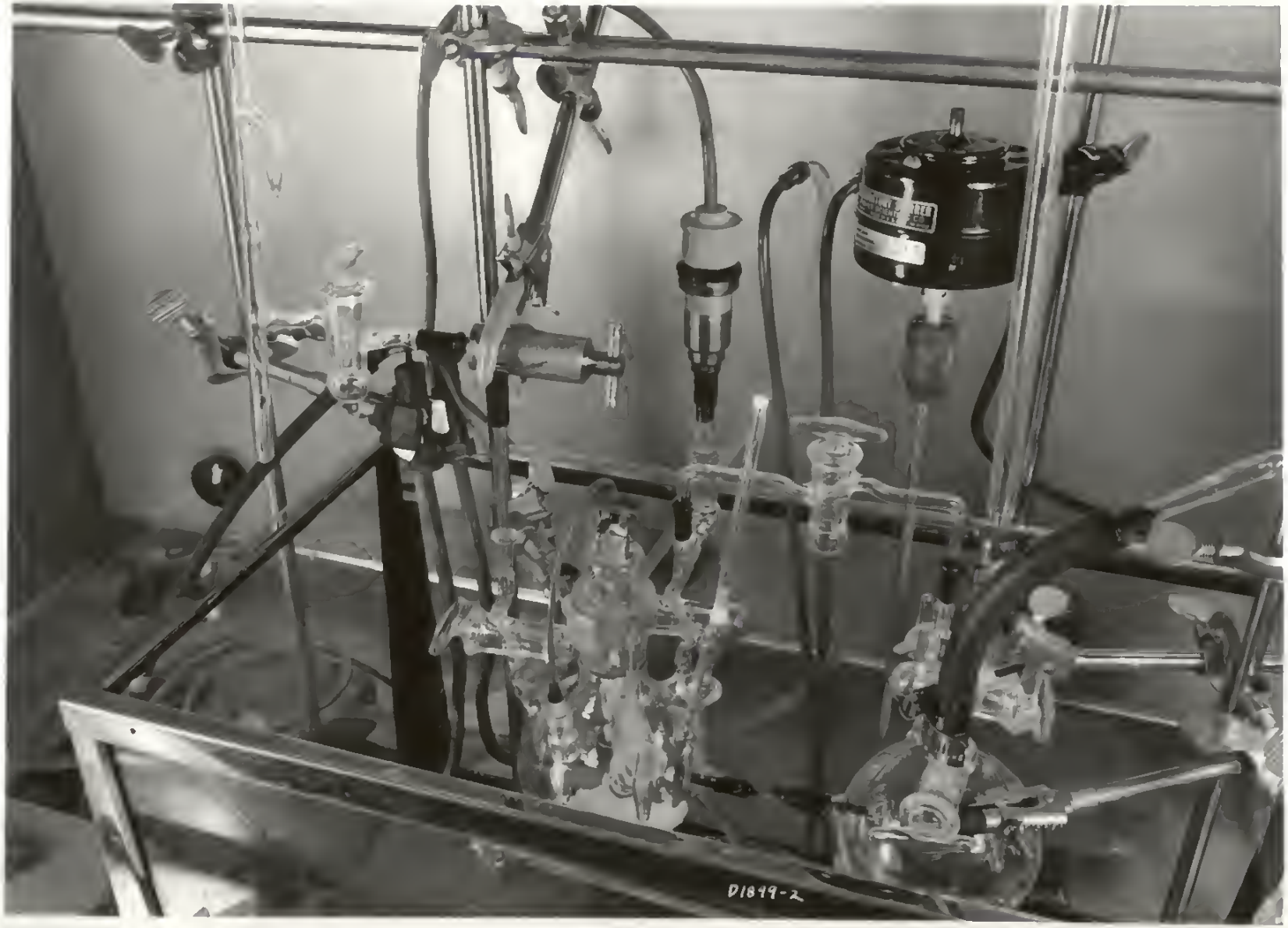

Figure 6. Assembly of diffusion cell apparatus (electrical and light shields not shown).

Figure 7. Surface-barrier radiation detector before insertion into operating position.

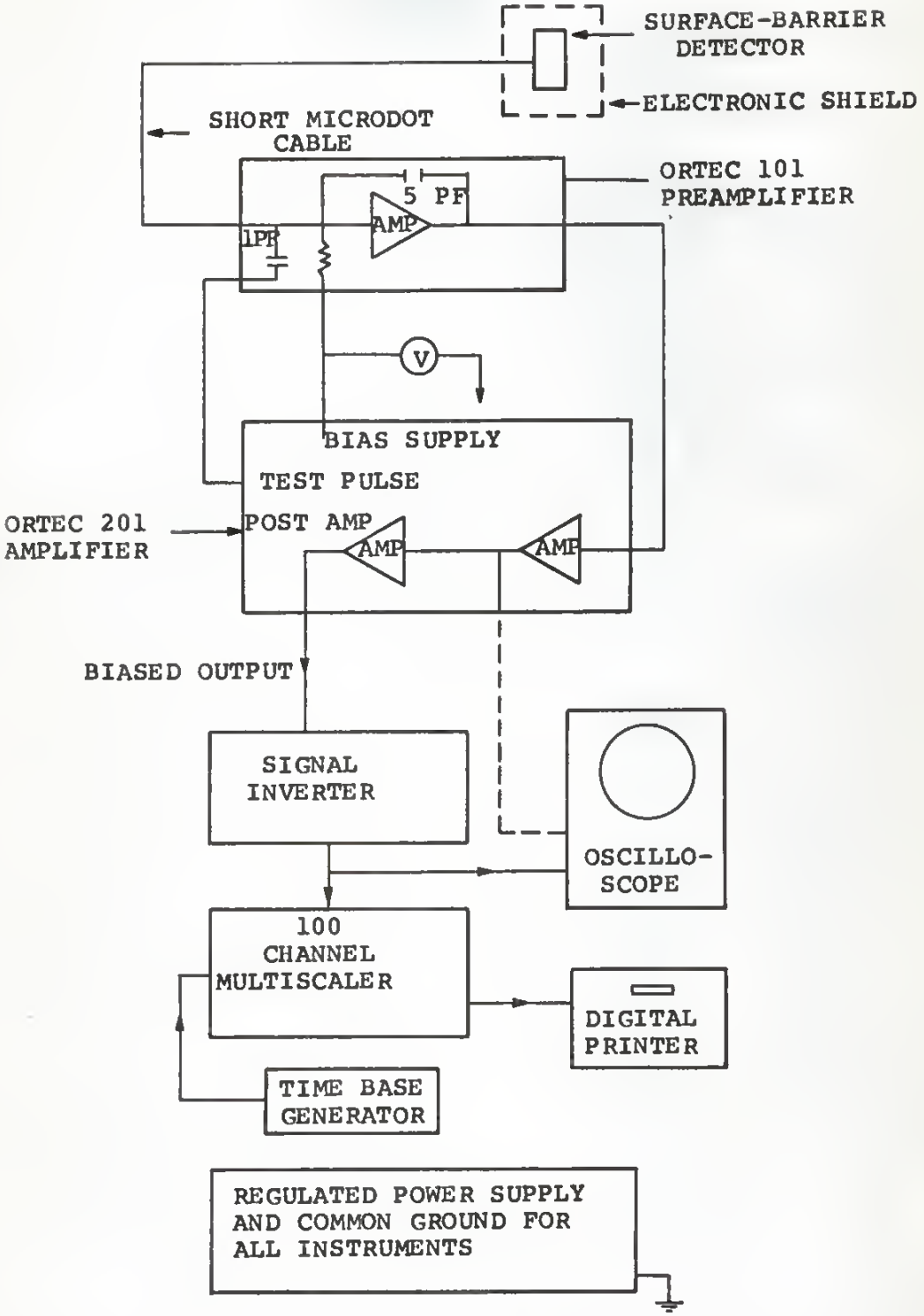

Figure 8. Block diagram of complete counting system.

radiation detector. The detector was installed in flask I, suspended from two No. 22 tungsten wire leads passing through a removable ₹ 34/45 ground glass stopper. The capillary tube and a pressure equalization tube "11" provided vacuum tight connections between flask I and flask II. The length and the internal diameter of the precision bore capillary tube were found to be 10.00 cm and 0.1026 cm respectively. The diameter was determined by measuring the length and mass of a thread of mercury inside the tube. High vacuum stopcocks were used to control gas flow through the six orifices in flask I and II, through the pressure equalization tube, and to the thermocouple vacuum gauge tubes, "6" and "18" (See Appendix B for detailed experimental procedure). Flasks I and II had volumes of 579 and 512 ml, respectively. The capacities of these flasks, up to the bottom of the ground glass joint (see Fig. 2), were determined by filling with a measured quantity of water.

A stiff molybdenum wire passing through a spherical ground glass joint provided a lever arm for operation of the capillary tube valve "10". A small conical piece of soft rubber was attached to the end of the wire so that it entered and sealed the end of the capillary tube when the valve was in the closed position. This capillary tube valve, which differed from those of many earlier experimental diffusion arrangements, was designed to prevent any discontinuities or irregularities along the diffusion path.

Radioactive and nonradioactive gas flowed to flask I through stopcocks "4" and "9" respectively. The nonradioactive gas (greater than 99.5% pure) was purified in a tube of Drierite, silica gel, and magnesium perchlorate. Volk Radiochemical Company supplied glass ampoules of both $C^{14}O_2$ and $C^{14}H_4$. The specific activity of the $C^{14}O_2$ was 1 millicurie/millimole (0.01% vol $C^{14}O_2$) and the ampoule contained 0.10 mc of $C^{14}O_2$. The total activity of the ampoule of $C^{14}H_4$ was 0.5 mc of $C^{14}H_4$ and the specific activity was 5 mc/mm (0.05% vol $C^{14}H_4$). After the diffusion cell was purged with nonradioactive gas, trace gas was throttled into flask I through the Hoke needle valve "3".

A two station Cenco vacuum gauge (Type GMA-140) was utilized in measuring pressures in the flasks. By closing "11", the pressure in flask I was measured by gauge tube "6" with valve "5" open; the pressure in flask II was measured by gauge tube "18" with "11" closed and "13" open.

An upright McLeod vacuum gauge, "14", (range 0.05 to 500 microns) connected to flask II was used in calibrating the thermocouple gauge. For methane quadratic relationships were found for the calibrations between gauge readings and absolute pressure in the range of interest (0-500 microns). The vacuum gauge meter could be read to approximately $\pm$1% between 0 and 100 microns and to $\pm$5% at higher pressures.

A 12 gallon tank filled with water served as a constant temperature (20°C) bath for the diffusion cell (95% immersed). Constant temperature regulation to $\pm$0.1°C. was provided by a

thermoregulator and relay which controlled a low wattage heating element. Tap water (16.5°C) running through a coiled copper tubing served as the heat sink.

The diffusion cell, together with all auxiliary equipment containing radioactive gas, was housed in a high velocity hood to guard against exposure to radiation. A liquid nitrogen trap installed between stopcock "13" and the two-stage, oil sealed mechanical vacuum pump prevented the escape of radioactive gas through the pump exhaust. The cold trap was periodically removed to allow accumulated solids to sublime and be expelled slowly through the hood exhaust.

2.5.2 Electronic Counting System

The ability of an electronic counting system to detect low energy beta particles, such as those emitted by carbon-14 (E_{max} = 156 kev (40)) has been shown to be dependent upon the signal to noise ratio of the amplified detector output. If noise amplitude is high compared to signal amplitude, it is usually not possible to separate the spurious counts from those that are real. If, on the other hand, the signal-to-noise ratio is large it is possible to electronically discriminate against the noise pulses and count only the pulses produced by radiation incident upon the detector. For the case of polyenergetic C^{14} beta particle detection, part of the real signal is always discriminated out with the noise. Thus, the detection system used in this experiment

was designed to develop a minimum amount of noise. It is most important that the production of noise is prevented at that point in the counting system where the real signal is the smallest, i.e., at the detector where the signal is created.

Because the surface-barrier radiation detector was extremely sensitive to electromagnetic radiation, it was necessary to construct an electrical and a light shield surrounding the glass flask housing the detector. A fine-mesh brass screen jacket built around flask I (see Fig. 5) and grounded to the preamplifier chassis was effective in shielding against stray electrical signals. The complete outer surface of flask I, except for small parts of stopcocks "4", "5", and "9", was painted with black Glyptal paint. Since the capillary tube served as a light pipe between the two flasks, part of flask II was also painted. Detector surface leakage was avoided by handling the detector with extreme care. Thermal noise in the detector was minimized by maintaining the detector at a constant temperature.

A five inch long microdot shielded cable connected the detector leads to an ORTEC low noise preamplifier (Model 101). This cable was made as short as possible to reduce input capacitance since the signal voltage was inversely proportional to the sum of the effective detector capacitance and all other input capacitances. The preamplifier utilized a charge-sensitive input circuit and a voltage amplifier provided with a negative feedback path allowing it to simulate a charge-to-voltage transducer.

Signals emerging from the preamplifier had an amplitude of several millivolts.

The preamplifier was connected to the ORTEC low noise amplifier (Model 201) through a shielded cable. This amplifier chassis contained the power supplies, the 60 cycle test pulse generator, the discriminator bias circuit, and the main and post amplifiers. A Tektronix oscilloscope (Type 515A) was used to monitor the amplified signal and thereby select proper adjustments for the amplifiers. The positive signal output of the post amplifier was inverted and attenuated by a EG & G IT 100 inverting transformer to make it compatible with the TMC Gammascope II (Model 102) multichannel analyzer (scaler mode).

A square wave from a Krohn-Hite low frequency generator (Model 400-C) was used as the external time base for the analyzer. The wave frequency was variable between 0.009 and 1100 cycles per second. The paper tape containing the experimental data was printed with a Hewlett-Packard digital recorder (Model 561-B). Serious ground loop and line transient problems were alleviated by connecting all electronic equipment, excluding the scope, to a well regulated Beckman power supply.

2.6.0 Reduction of Data

2.6.1 Preparation of Data for Analysis

The method of analysis of data in this study was basically the same as that presented by Mistler (53). It consists of an

iterative least squares fitting of the data to determine the effective diffusion coefficient. A description of this analysis and the computer program used to perform it is given in Appendix C.

The only steps required to ready the data for computer treatment were determination of the average initial and final count rates and the deletion of data points which were obviously in error. The average initial count rate was found by simply averaging the data points taken before opening the capillary tube valve, while the final average count rate was the average of data points taken after the system reached equilibrium. The deletion of some data points within a run was sometimes necessitated because the values for these points were obviously much too large. The gross errors of these values were caused by vibration of the system and detector upon opening the capillary valve or by the electronic pickup of electromagnetic noise. For the data of a run to be considered reliable the number of such points encountered was severely restricted. A sample set of data taken at a pressure of 203 μ is shown in Table I. An application of least squares analysis and the mass correction for isotopic self-diffusion to this data indicated a value of $D_{e_{11}} = 614.3 \pm 14.4$ cm^2/sec. It is noted that the diffusion coefficient actually measured was the mutual diffusion coefficient for the two isotopes. Throughout the analysis, however, this was assumed to be equal to the self-diffusion coefficient of the natural gas. The mass correction factor was applied as a final step.

Table I. Sample set of count-rates versus time data taken from the analyzer output.

Time[a] (sec)	Counts/Channel	Time (sec)	Counts/Channel
0	1693	754	1106
29	1654	774	1069
49	1667	793	1097
69	1652	813	1061
88	1561	832	1096
108	1516	852	1054
127	1490	871	1112
147	1483	891	1057
166	1562	911	1077
186	1547	930	1148
206	1505	950	1036
225	1398	969	1010
245	1392	989	1057
246	1378	1028	1059
284	1405	1048	1042
304	1246	1067	1032
323	1481	1087	1048
343	1361	1106	1021
362	1316	1126	1125
382	1272	1148	951
401	1289	1165	1048
421	1247	1185	970
441	1288	1204	1006
460	1297	1224	1004
480	1210	1244	1008
499	1266	1263	1000
519	1202	1283	955
539	1156	1302	1000
558	1220	1322	970
578	1181	1341	925
597	1147	1361	993
617	1209	1381	973
636	1177	1400	973
656	1167	1420	976
676	1111	1439	1011
695	1209	1459	949
715	1166	1479	947
734	1139	1498	956

Table I (Continued)

Time (sec)	Counts/Channel	Time (sec)	Counts/Channel
1518	918	1635	955
1537	1003	1655	974
1557	976	1674	957
1576	887	1694	941
1596	920	1714	896
1616	913	1733	967

P = 203 μ

Initial pressure difference = -2 μ

$D_{e_{11}}$ before pressure-induced flow correction = 614.3

Deviation arising only from least squares analysis = 12.1

Combined deviation caused by least squares and uncertainty of pressure measurement = 14.4

$D_{e_{11}}$ after correction for pressure-induced flow = 617.4

[a]The measured time increment was 19.583 sec.; all the times above have been rounded to the nearest second.

2.6.2 Standard Deviation Analysis

For brevity, the effective mutual isotopic diffusion coefficient, D_{e12}, is referred to merely as "D" in this section. The uncertainty associated with the determination of the diffusion coefficient was the result of scatter in the measured count rates, a negligible error in time measurements and uncertainty in measurements of pressure. Assuming a normal distribution for errors in the measurement of count rates an expression for this uncertainty in D may be found.

Given the relationship

$$X = f(t,D) \tag{32}$$

where D is a dependent variable of the measured quantities X and t, the error of D due to errors in measurement is given by the theory of propagation of errors. Letting D equal diffusion coefficient, t equal time, X equal normalized count rate, and variances of the quantities X, D, and t equal σ_x^2, σ_D^2, and σ_t^2, respectively the relationship given is

$$\sigma_x^2 = \left(\frac{\partial f(t,D)}{\partial D}\right)^2 \sigma_D^2 + \left(\frac{\partial f(t,D)}{\partial t}\right)^2 \sigma_t^2 \tag{33}$$

Since σ_t^2 can be set equal to zero if the measurement of t has negligible error, the variance of D calculated from N data points is given as

$$\sigma_D^2 = \sigma_x^2 \left[\sum_{i=1}^{N} \left(\frac{\partial f(t,D)}{\partial D}\right)^2\right]^{-1} \tag{34}$$

Brownlee (9) has presented a theory for an estimate of σ_x^2 based upon the residuals between the least squares fit and the data. The best estimate of the variance of X is given by

$$\sigma_x^2 = (N-c)^{-1} \sum_{i=1}^{N} (X_{ei}-X_{ei})^2 \tag{35}$$

where (N-c) = number of degrees of freedom associated with σ_x^2

c = number of variables, which was one for this analysis.

Thus, from Eqs. (34) and (35) the standard deviation for D is

$$\sigma_D(N) = \{(N-1)^{-1} \sum_{i=1}^{N} (X_{ei}-X_{ei})^2 [\sum_{i=1}^{N} (\frac{\partial f(t,D)}{\partial D})^2]^{-1}\}^{1/2} \tag{36}$$

where the dependence upon the number of data points N is explicitly noted and before the uncertainty arising from pressure measurements is considered.

It should be noted that the measurement of pressure does not enter directly into the determination of D. However, pressure is the independent variable reported with D values and with which they are plotted. Although results could be reported showing uncertainties in both the diffusion coefficient and the pressure, it is desirable to report them in the conventional manner with an uncertainty associated entirely with the dependent variable, D. To determine this equivalent description of variance, it is assumed that the total variance of D is the sum of that originating in the least squares analysis and the variance associated with the uncertainty in the pressure measurements. An estimate of the

latter quantity is obtained by assuming Bosanquet's relationship to be true

$$D \approx D_{e11} = [1/D_{K_1} + 1/D_{11}]^{-1}$$

$$= D_{K_1} D_{B_1}/(D_{B1} + D_{K_1}P) \qquad (37)$$

where D_{K_1} = the Knudsen diffusion coefficient, cm^2/sec

D_{B1} = the diffusion coefficient at atmospheric pressure, cm^2/sec

P = the pressure, atm.

Assuming a normal propagation of error, Eq. (33) may then be applied to yield

$$\sigma_D{}^2(P) = [D_{B1} D_{K1}^2/(D_{B1} + D_{K1}P)^2]^2 \sigma_P{}^2$$

$$= [D_{e11}^2/D_B]^2 \sigma_P{}^2 \ . \qquad (38)$$

The value of D_{e11} is obtained from Eq. (37).

In order to estimate the values of $\sigma_P{}^2$, the absolute pressure was expressed in terms of polynomial functions of the pressure gauge readings. The parameters of these functions and the variances of the parameters were found by use of POLYFIT (19), a least squares, polynomial fitting computer program. The order of polynomial to be used for the description of a calibration curve was selected on the basis of the location of a local minimum in plots of quality of fit number versus order of fit. It should be noted that actual pressure determinations were made directly from

calibration curves. Use of the describing functions was restricted to estimation of the variance of the experimental diffusion coefficient. By use of these functions and again the assumption of a normal propagation of error, an absolute pressure value and an associated variance could be found for a given pressure gauge reading.

Knowledge of σ_p^2 and D_{ell} allow the evaluation of Eq. (38) to give an estimate of the variance of D caused by uncertainty of pressure measurements. The deviation of the effective diffusion coefficient is finally given as the square root of the sum of the variance originating in the least squares analysis of count rate-time data and the variance given by Eq. (38) as

$$\sigma_D = \{\sigma_D^2(N) + \sigma_D^2(P)\}^{1/2} \qquad (39)$$

3.0 RESULTS AND DISCUSSION

3.1 General Discussion

The purpose of this study was to verify and extend the work of Mistler (53) and to refine and further demonstrate the feasibility of the experimental and analytical techniques he employed. A modified Ney-Armistead cell was used with a tracer technique which utilized a semiconductor radiation detector within the cell. Effective gaseous self-diffusion coefficients were measured in the transition pressure range. This pressure range was chosen because of the great scarcity of diffusion data for it. The results given in this section illustrate the success of the study in achieving these goals. In particular, the CO_2 data represents the results of improvements in experimental apparatus and was taken to substantiate Mistler's results. In addition data for methane was obtained.

Experimentally determined values of the self-diffusion coefficient for CO_2 in the transition pressure range at 20°C are presented in Table II and Fig. 9. Values for CH_4 are shown in Table III and Fig. 10. The results for each gas have been compared with theoretical values predicted by the relationships of Bosanquet and Wheeler, Eq. (19) and Eq. (24) respectively. Values of D_{11} in the theoretical calculations were derived from the theory of Chapman and Cowling (12) at 760 mm pressure and 20°C. For CO_2, the theoretical self-diffusion coefficient under these

Table II. Experimental and theoretical results for the self-diffusion coefficient of carbon dioxide in the transition pressure range.

P Microns of Hg	D_e (cm^2/sec) Experimental self-diffusion	D_e (cm^2/sec) Bosanquet	D_e (cm^2/sec) Wheeler
46	718.1 ± 45.5	735	899
104	567.5 ± 24.2	484	628
204	348.2 ± 14.1	304	384
306	257.7 ± 9.1	221	266
442	222.3 ± 6.1	162	186
451	194.1 ± 6.1	159	182

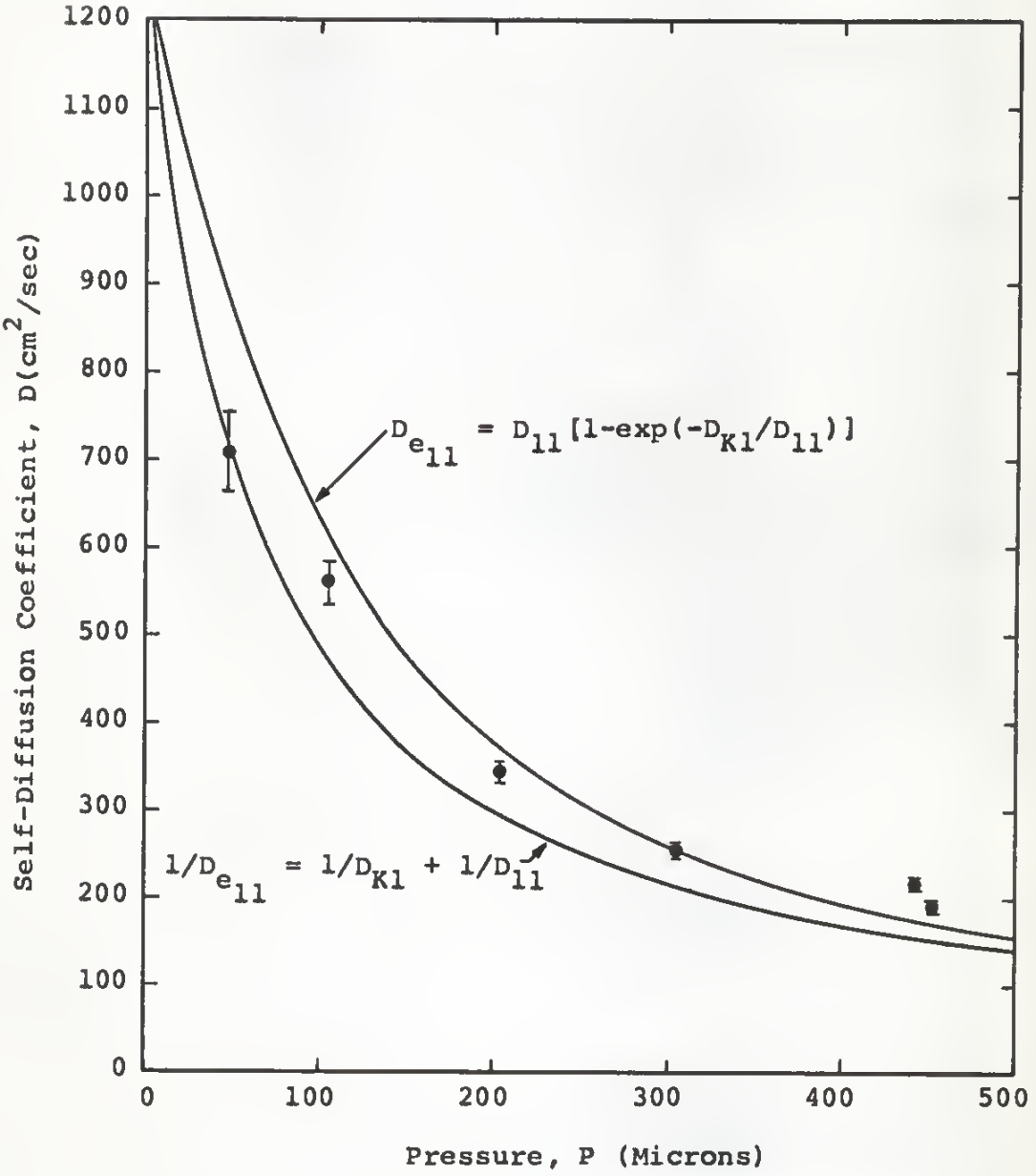

Figure 9. Comparison between experimental and theoretical self-diffusion coefficients for CO_2.

Table III. Experimental and theoretical results for the self-diffusion coefficient of methane in the transition pressure range.

P Microns of Hg	D_e (cm^2/sec) Experimental self-diffusion	D_e (cm^2/sec) Bosanquet	D_e (cm^2/sec) Wheeler
47	1184.3 ± 35.0	1290	1570
52	1102.8 ± 35.0	1240	1520
53	1162.6 ± 45.4	1230	1510
74	1018.0 ± 21.6	1050	1330
78	963.6 ± 25.7	1030	1300
80	1028.7 ± 24.7	1010	1290
102	988.0 ± 37.0	885	1140
108	842.1 ± 20.6	856	1110
127	777.4 ± 20.3	774	1000
150	707.0 ± 18.1	694	900
157	656.7 ± 19.6	673	871
175	659.5 ± 17.1	624	804
198	632.1 ± 16.5	571	730
203	614.3 ± 14.4	561	715
251	547.8 ± 14.4	478	596
308	586.1 ± 8.0	406	495
352	445.6 ± 7.4	364	436
396	382.0 ± 8.3	330	389
500	322.9 ± 6.2	270	309

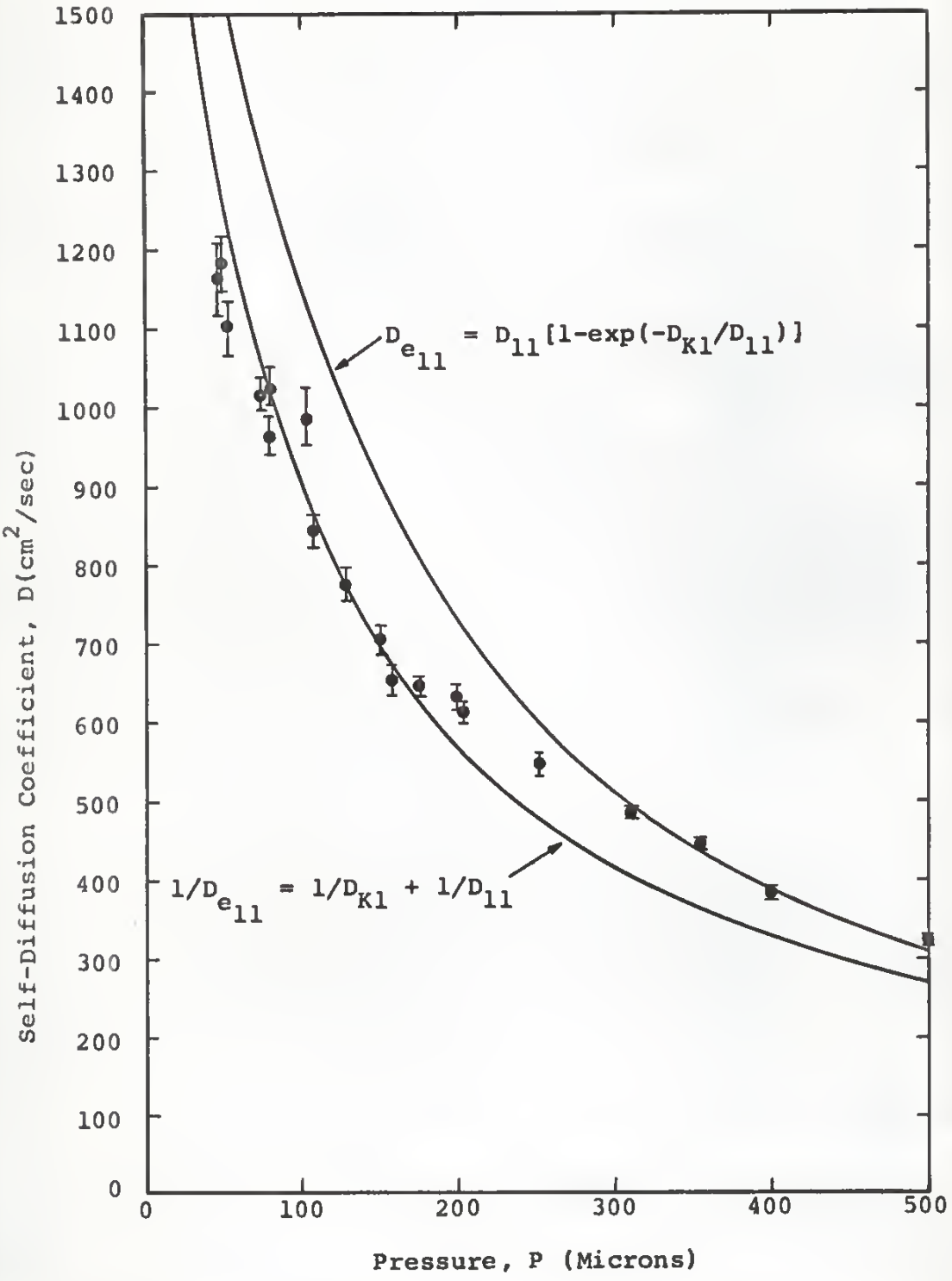

Figure 10. Comparison between experimental and theoretical self-diffusion coefficients for CH_4.

conditions was 0.102 $cm^2/sec.$; for CH_4 it was found to be 0.203 cm^2/sec. The Knudsen coefficients were found from Eq. (11) for the .1026 cm I.D. capillary tube. They were 1284 and 2127 cm^2/sec for CO_2 and CH_4, respectively. The reported values of D_{e11} were calculated by Eq. (25) using experimental values of D_{e12}, the diffusion coefficient of the tracer gas in the natural gas. For $C^{14}O_2$ in CO_2 the correction factor was 1.011 while for $C^{14}H_4$ in CH_4 it was 1.029.

The deviation reported for each experimental diffusion coefficient was the standard deviation which corresponds to 67% confidence limits. This deviation is a measure of the accuracy of the least squares fit of the data and of the uncertainty of pressure measurements. For the CO_2 data the error represented by these deviations ranges from 6.4% for the measurement at 46 microns to 2.7% for the measurement at 442 microns. For CH_4 the percentage deviations range generally from 2-3% with only an occasional instance as high as 5.5% at pressures of approximately 50 microns. These deviations do not include the effect of error in measuring system parameters.

The agreement of the experimental results for CO_2 with theoretical values is shown in Fig. 2. At the lowest pressure investigated, 46 microns, the experimental value is seen to be in excellent agreement with the theoretical prediction by Bosanquet. At intermediate pressures they lie within the band between the two theoretical curves. With increasing pressure the experimental values exceed those predicted by Bosanquet by increasing

percentages. This general trend agrees with that found by Mistler. It is thought to be explained to some degree by the occurrence of surface diffusion. This phenomenon occurs by the mechanism of molecular transport with an absorbed layer on the surface of the capillary tube. Transport by surface diffusion is complementary to diffusion occurring in the gaseous phase and its effect would be to increase the observed effective diffusion coefficient. Discussions of this phenomenon are presented by Reynolds and Richley (64,65), Clausing (13), Hill (35), and others (11,13,18, 35,57,68,88).

The agreement of experimental results for CH_4 with the theoretical curves is shown in Fig. 3. The same general trend is noted in the CH_4 data. At low pressures the agreement with Bosanquet's relationship is rather good although the points tend to lie somewhat below the theoretical curve. No explanation for this tendency is readily available. At intermediate pressures the measured values again lie within the region between the two theoretical curves; however, this behavior occurs at higher pressures than for CO_2. Finally at the upper pressure region of the transition range the measured values consistently exceed the values of Bosanquet's relationship. Again this is thought to be explained to some extent by surface diffusion.

The occurrence of surface diffusion is thought to account for the largest single source of experimental error. At the present time, knowledge of this phenomenon is largely restricted to very generalized theoretical results (64) or to studies of

very specialized cases. No attempt was made to analyze its quantitative effects in this study.

Pressure control and measurement also were responsible for some error in the determinations which is represented by $\sigma_D(P)$ and is included in the reported standard deviation. This uncertainty in pressure measurement generally accounted for less than 30% of the total deviation. The procedure for this analysis is explained in Section 2.6.2.

The presence of a pressure gradient between the two flasks would of course result in an erroneous measurement of the diffusion coefficient. By use of pressure gauges in both flasks this problem was essentially eliminated. Analysis of this source of error by the approximation presented in Appendix E indicated that it contributed an error of considerably less than 1% to the reported values.

Mistler (53) has presented a study of errors caused by inaccuracies in the measurement of system parameters and in general these errors were found to be small in comparison with the counting error associated with the reported standard deviation.

A final possible source of error is the Rayleigh end-correction which was used for determining the effective tube length. Although this is the accepted method of correction, it does not allow for expected changes in the diffusion length as Knudsen diffusion becomes predominant. Presently no relationship has been accepted for the change in effective tube length as a function of pressure.

3.2 Conclusion

Comparison of the results presented above with the stated purposes of the study allow some conclusions to be drawn.

Refinements in Mistler's experimental equipment have reduced the importance of and, in some cases, eliminated sources of potential error. Refinements in the analysis of data have permitted more meaningful estimates of errors. The small amount of CO_2 data presented was in good agreement with Mistler's. This indicates that results are reproducible. The feasibility of using a semiconductor detector in a modified Ney-Armistead diffusion cell to measure diffusion coefficients has been further demonstrated by the investigation of the $C^{14}H_4$-CH_4 system. Effective self-diffusion coefficients of CH_4 at pressures from 50 to 300 microns were found to compare within 10% with the theory of Bosanquet.

Although the refinement of this method must be considered incomplete, the results of this study suggest that further efforts will produce a useful research tool for determination of effective diffusion coefficients in the transition pressure range.

4.0 SUGGESTIONS FOR FURTHER STUDY

A first step in the extension of this study would be a thorough investigation of the effects of surface diffusion. It is believed that modification of the mathematical model to include these effects would eliminate a major source of error. The use of more precise pressure measuring devices would be highly desirable. The determination of system parameters could be improved by measuring the volumes of the flasks after final assembly with a gas instead of a liquid; the capillary tube radius could be determined more accurately by optical or viscosity measurements, particularly if its bore were smaller. Efforts should be made to obtain more precise temperature control, preferably $\pm 0.01°$ C. If possible, future studies should employ tracer gas of a higher specific activity to reduce errors produced by low count rates. The length of the capillary tube should be varied in order to extend the pressure range to be investigated. This would also allow the determination of an end-correction for the tube length as a function of pressure.

Other possibilities for modification of the apparatus include the installation of detectors in both flasks. This change coupled with a mathematical solution in which the tube volume is considered negligible would greatly simplify data analysis, and allow several measurements within a run. It would however complicate the supporting electronic system.

An exact mathematical solution or method of numerical analysis for the system under conditions of simultaneous diffusion

and pressure induced flow would not only simplify the demands of the experimental procedure, but would also allow the measurement of other transport properties, such as an effective transition range viscosity.

The possibilities for study of other gaseous systems are almost unlimited. Included in these are the measurement of self-diffusion coefficients for other gases, the measurement of mutual diffusion coefficients for binary mixtures, and determinations of the concentration dependence of mutual diffusion coefficients. By use of multiple tracers and pulse height analysis studies could be performed in multicomponent systems.

5.0 ACKNOWLEDGEMENT

The author wishes to express his appreication to the faculty and staff of the Nuclear Engineering Department. In particular, sincere gratitude is extended to:

Dr. J. O. Mingle, who originated this study, for his guidance, advice, and constructive criticisms.

Dr. W. R. Kimel, Head of the Department of Nuclear Engineering, for his continued assistance and guidance.

The Kansas State University Engineering Experiment Station and the Petroleum Research Fund of the American Chemical Society for their financial support.

The Atomic Energy Commission, who through their fellowship program, have made the opportunity of this study possible.

6.0 LITERATURE CITED

1. Adzumi, H.
   Studies in the Flow of Gaseous Mixtures through Capillaries. Bull. Chem. Soc. Japan, 12, 285 (1937).

2. Amdur, I. and T. F. Schatzki
   Diffusion Coefficients of Systems Xe-Kr and A-Xe. J. Chem. Phys., 27, 1049 (1957).

3. Bendt, Phillip J.
   Measurements of He^3-He^4 and H_2-D_2 Gas Diffusion Coefficients. Phys. Rev., 110, 85 (April 1958).

4. Boardman, L. E. and N. E. Wild
   The Diffusion of Pairs of Gases with Molecules of Equal Mass. Proc. Roy. Soc. (London), 162A, 511 (1937).

5. Bohemen, J. and J. H. Purnell
   Diffusional Band Spreading in Gas-Chromatographic Columns, I. J. Chem. Soc., 360 (1961).

6. Bosanquet, C. H.
   British TA Report. BR-507 (Sept. 1944).

7. Boyd, Charles, Norman Stein, Virginia Steingrimsson, and William R. Rumpel
   An Interferometric Method of Determining Diffusion Coefficients in Gaseous Systems. J. Chem. Phys., 19, 548 (1951).

8. Brown, C. C.
   Solid State Radiation Detectors. Nuclear Science, IRE Transactions on Nuclear Science, 8, 331 (Jan. 1961).

9. Brownlee, K. A.
   Statistical Theory and Methodology in Science and Engineering. (John Wiley & Sons, Inc., New York, 1965), 2nd Edition.

10. Buckingham, E.
    Contributions to Our Knowledge of the Aeration of Soils. U. S. Dept. Agr., Bur. Soils, Bull. No. 25 (1904).

11. Carman, Philip Crosbie
    Flow of Gases Through Porous Media. Academic Press, Inc. (1956).

12. Chapman, Sidney and T. G. Cowling
    Mathematical Theory of Non-uniform Gases. (Cambridge University Press, Cambridge, Mass., 1952), 2nd Edition.

13. Clausing, P.
The Flow of Very Dilute Gases Through Tubes of Any Length. Ann. Phys., 12, 961-989 (March 10, 1932).

14. Coward, H. F. and E. H. M. Georgeson
The Diffusion Coefficient of Methane and Air. J. Chem. Soc., 2, 1085 (1937).

15. Crank, J.
The Mathematics of Diffusion. (Claredon Press, Oxford, 1956).

16. Crawford, G. E.
Semiconductors as Radiation Detectors. Nuclear Power, 4, 84 (August 1959).

17. Dearnaley, G. and N. C. Northrop
Semiconductor Counters for Nuclear Radiations. (John Wiley & Sons, Inc., New York, 1963).

18. Dykman, I. M.
On the Mechanism of Activator Vapor Supply to the Outer Surface of a Porous Metal-Film Cathode. Radio Engl. and Electronics Phys., 2, 83-89 (1957).

19. Eckhoff, N. D., T. R. Hill and W. R. Kimel
Trace Element Determinations by Neutron Activation Analysis: Theory and Development. 99th Annual Meeting, Kansas Academy of Sciences, Salina, Kansas (May 4-5, 1967).

20. Ember, G., J. R. Ferron and K. Wohl
A Flow Method for Measuring Transport Properties at Flame Temperatures. A.I.Ch.E. Journal, 10, 68 (1964).

21. Evans, E. V. and C. N. Kenney
Gaseous Dispersion in Laminar Flow through a Circular Tube. Proc. Roy. Soc., A284, 540 (1965).

22. Evans, R. B., III, G. M. Watson, and E. A. Mason
Gaseous Diffusion in Porous Media at Uniform Pressure. J. Chem. Phys., 35, 2076-2083 (Dec. 1961).

23. Evans, R. B., III, J. Truitt, and G. M. Watson
Superposition of Forced and Diffusive Flow in a Large-Pore Graphite. ORNL-3067 (1961).

24. Fairstein, E. and J. Hahn
Nuclear Pulse Amplifiers--Fundamentals and Design Practice. Nucleonics, 23, 56 (July 1956).

25. Friend, Leo and Stanley B. Adler
Transport Information Needed in the Chemical and Process Industries. Transport Properties in Gases. (Northwestern University Press, Evanston, Illinois, 1957).

26. Gaede, W.
Ann. Physik, 41, 289 (1913).

27. Giddings, J. Calvin and Spencer L. Seager
Method for Rapid Determination of Diffusion Coefficients. Industrial and Engineering Chemistry Fundamentals, 1, 277 (1960).

28. Giddings, J. C. and S. L. Seager
Rapid Determination of Gaseous Diffusion Coefficients by Means of Gas Chromatography Apparatus. J. Chem. Phys., 33, 1579 (1960).

29. Giddings, J. C. and S. L. Seager
Coiled Columns and Resolution in Gas Chromatography. J. Chromatog., 3, 520 (1960).

30. Giddings, J. C., S. L. Seager and L. R. Geerston
Temperature Dependence of Gas and Vapor Diffusion Coefficients. J. Chem. Eng. Data, 8, 168 (1963).

31. Goulding, R. S.
Semiconductor Detectors--Their Properties and Applications. Nucleonics, 22, 54 (May 1964).

32. Groth, W. and P. Harteck
Z. Electrochemi, 47, 167 (1941).

33. Harteck, P. and H. W. Schmidt
Z. Physik, Chem., 21B, 447 (1932).

34. Hildebrand, F. B.
Introduction to Numerical Analysis. (McGraw-Hill Book Company, New York, 1956).

35. Hill, Terrell L.
Surface Diffusion and Thermal Transpiration in Fine Tubes and Pores. J. Chem. Phys., 25, 730-735 (Oct. 1956).

36. Hirschfelder, J. O., C. F. Curtiss, and R. B. Bird
Molecular Theory of Gases and Liquids. (John Wiley & Sons, Inc., New York, 1954).

37. Hofstadter, R.
Crystal Counters. Part I. Nucleonics, 4 (April 1949).

38. Hofstadter, R.
Crystal Counters. Part II. Nucleonics, 4 (May 1949).

39. Hutchinson, Franklin
Self Diffusion in Argon. J. Chem. Phys., 17, 1081 (1941).

40. Jeffries, Q. R. and H. G. Drickamer
Diffusion in CO_2-CH_4 Mixtures to 225 Atm. J. Chem. Phys., 22, 436 (March 1954).

41. Johnson, E. F.
Molecular Transport Properties of Fluids. Ind. Eng. Chem., 45, 902 (May 1953).

42. Johnson, E. F.
Molecular Transport Properties of Fluids. Ind. Eng. Chem., 47, 599 (March 1955).

43. Johnson, E. F.
Molecular Transport Properties of Fluids. Ind. Eng. Chem., 48, 582 (1956).

44. Jost, W.
Diffusion in Solids, Liquids and Gases. (Academic Press, Inc., New York, 1952).

45. Kelvin of Largs, Baron
Baltimore Lectures. (C. J. Clay & Sons, London, 1904), p. 293.

46. Knox, J. H. and L. McLaren
A New Gas Chromatographic Method for Measuring Gaseous Diffusion Coefficients and Obstructive Factors. Anal. Chem., 36, 1477 (1964).

47. Knudsen, Martin
Kinetic Theory of Gases. (John Wiley & Sons, Inc., New York, 1950), 3rd Edition.

48. Langmuir, I.
Evaporation, Condensation and Reflection of Molecules, and the Mechanism of Adsorption. Phys. Rev., 8, 149 (1916).

49. Langmuir, I.
Constitution and Fundamental Properties of Liquids and Solids. J. Am. Chem. Soc., 38, 2250 (1916).

50. Liley, P. E.
Survey of Recent Work on Viscosity, Thermal Conductivity and Diffusion of Gases. Progress in International Research in Thermodynamics and Transport Properties. (McGraw-Hill Book Company, New York, 1959).

51. Loschmidt, J.
Sitzb. Akad. Wiss. Wien., 61, 367 (1870).

52. Maxwell, J. C.
Electricity and Magnetism. (Dover Publications, New York, 1954), p. 434.

53. Mistler, T. E.
Radioactive Tracer Determinations of Gaseous Diffusion Coefficients. M.S. Thesis, Kansas State University, Manhattan, Kansas, 1966.

54. Ney, Edward P. and Fontaine C. Armistead
The Self-Diffusion Coefficient of Uranium Hexafluoride. Phys. Rev., 71, 14 (Jan. 1947).

55. O'Hern, H. A. and Joseph J. Martin
Diffusion in CO_2 at Elevated Pressures. Ind. Eng. Chem., 47, 2081 (1955).

56. Otani, Seiya, N. Wakao, J. M. Smith
Diffusion and Flow in Porous Catalysts. A.I.Ch.E. Journal, 11, 439.

57. Patterson, G. N.
A State-of-the-Art Survey of Some Aspects of the Mechanics of Rarefied Gases and Plasmas. Report No. ARL 64-60, Toronto University (April 1964).

58. Paul, Ranjit
Solutions of Concentration Dependent Diffusion Equation. Phys. Fluids, 3 (1960).

59. Pollard, W. G. and R. D. Present
On Gaseous Self Diffusion in Long Capillary Tubes. Phys. Rev., 73, 762 (April 1948).

60. Present, R. D.
Kinetic Theory of Gases. (McGraw-Hill Book Company, New York, 1958).

61. Price, W. J.
Nuclear Radiation Detection. (McGraw-Hill Book Company, New York, 1964), 2nd Edition.

62. Radeka, Veljko
Low Noise Preamplifiers for Nuclear Detectors. Nucleonics, 23, 52 (July 1965).

63. Rayleigh, Lord
Theory of Sound. Dover Publications, 2, 291 (New York), 1945.

64. Reynolds, T. W. and E. A. Richley
Analysis of Free-Molecule Flow with Surface Diffusion through Cylindrical Tubes. NASA TN D-3225, National Aeronautics and Space Administration, Washington, D. C. (1966).

65. Reynolds, T. W. and E. A. Richley
Free-Moledule Flow and Surface Diffusion through Slots and Tubes--A Summary. NASA TR R-255, National Aeronautics and Space Administration, Washington, D. C. (1967).

66. Rothfeld, Leonard B.
Gaseous Counterdiffusion in Catalyst Pellets. A.I.Ch.E. Journal, 9, 19 (Jan. 1963).

67. Scott, D. S. and F. A. L. Dullien
Diffusion of Ideal Gases in Capillaries and Porous Solids. A.I.Ch.E. Journal, 8, 113 (March 1962).

68. Sears, G. W.
A Note on the Flow of Gases Through Very Fine Tubes. J. Chem. Phys., 22, 1252-1253 (July 1954).

69. Sharpe, Jack
Nuclear Radiation Detectors. (John Wiley & Sons, Inc., New York, 1964).

70. Stefan, J.
Chemishes Zentralblatt, 42, 481 (1871); 44, 753 (1873); 49, 369, 721m (1878).

71. Strehlow, Roger A.
The Temperature Dependence of the Mutual Diffusion Coefficient for Four Gaseous Systems. J. Chem. Phys., 21, 2101 (1953).

72. Taylor, J. M.
Semiconductor Particle Detectors. (Butterworth, Washington, D. C., 1963).

73. Timmerhaus, K. D. and H. G. Drickamer
Self-Diffusion in CO_2 at Moderate Pressure. J. Chem. Phys., 19, 1242-1243 (1951).

74. Tordai, L.
Errors in Diffusion Measurements by Loschmidt Method. Br. J. Appl. Phys., 1, 329 (1950).

75. Visner, S.
Self-Diffusion in Capillaries at Low Pressures. Phys. Rev., 82, 297 (1951).

76. Volmer, M. and I. Estermann
Z. Physik, 7, 13 (1921).

77. Wakao, N. and J. M. Smith
Diffusion in Catalyst Pellets. Chem. Eng. Sci., 17, 825 (1962).

78. Walker, R. E. and A. A. Westenberg
New Method of Measuring Diffusion Coefficients of Gases. J. Chem. Phys., 29, 1753 (1957).

79. Walker, R. E. and A. A. Westenberg
Molecular Diffusion Studies in Gases at High Temperature, I and II. J. Chem. Phys., 29, 1139 and 1147 (1958).

80. Walker, R. E. and A. A. Westenberg
Molecular Diffusion Studies in Gases at High Temperature, III. J. Chem. Phys., 31, 519 (1959).

81. Walker, R. E. and A. A. Westenberg
Measurements of Multicomponent Diffusion Coefficients for the CO_2-He-N_2 System Using the Point Source Technique. J. Chem. Phys., 32, 1314 (1960).

82. Wheeler, Ahlborn
Advances in Catalysis. Academic Press, 3, 249 (New York), 1951.

83. Winn, E. B. and E. P. Ney
The Determination of the Self-Diffusion Coefficient of Methane. Phys. Rev., 72, 77 (1947).

84. Winn, E. B.
Self-Diffusion Coefficient of Nitrogen. Phys. Rev., 74, 698 (1948).

85. Winn, E. B.
The Temperature Dependence of the Self-Diffusion Coefficients of Argon, Neon, Nitrogen, Oxygen, and Methane. Phys. Rev., 80, 1024 (1950).

86. Winter, E. R. S.
Diffusion Properties of Gases. Transactions of Faraday Society, 46, 81 (1950).

87. Winter, E. R. S.
Diffusion Properties of Gases, Part IV. Transactions of Faraday Society, 47, 342 (1951).

88. Winterbottom, W. L. and J. P. Hirth
Diffusional Contribution to the Total Flow from a Knudsen Cell. J. Chem. Phys., 37, 784-793 (August 15, 1962).

7.0 APPENDICES

7.1 APPENDIX A

Solution to the Differential Equation for Diffusion Through a Capillary Tube

Based upon the assumption that Fick's second law is valid for the process of gaseous diffusion in a capillary tube, the partial differential equation which described gaseous diffusion in the system under study was

$$\frac{\partial C}{\partial t} = D \frac{\partial^2 C}{\partial z^2} . \tag{A-1}$$

In this section, Eq. (A-1) is solved by the method of Laplace transforms for the three following boundary conditions:

$$t = 0, \quad z > 0, \quad C = C_1 \tag{A-2}$$

$$t > 0, \quad z = 0, \quad C\Big|_{z=0} = C_o - V_1^{-1}\int_0^t (-D\pi R^2)\frac{\partial C}{\partial z}\Big|_{z=0} dt \tag{A-3}$$

$$t > 0, \quad z = L, \quad C\Big|_{z=L} = C_1 + V_2^{-1}\left(\int_0^t (-D\pi R^2) \frac{\partial C}{\partial z}\Big|_{z=0} dt \right.$$

$$\left. - \int_0^L \pi R^2 C dz + C_1 \pi R^2 L\right) \tag{A-4}$$

To transform Eq. (A-1) and the boundary conditions to dimensionless equations let $X = C/C_o$, $\xi = z/L$, and $\tau = tD/L^2$. These definitions, when applied to the format of Eqs. (A-1), (A-2), (A-3), and (A-4), yield

$$\frac{\partial X(\tau,\xi)}{\partial \tau} = \frac{\partial^2 X(\tau,\xi)}{\partial \xi^2} , \tag{A-5}$$

while the boundary conditions become

$$\tau = 0, \quad \xi > 0, \quad X = X_1 \tag{A-6}$$

$$\tau > 0, \quad \xi = 0, \quad X = 1 - \alpha\int_0^\tau \frac{\partial X(\tau,0)}{\partial \xi}\, d\tau \tag{A-7}$$

$$\tau > 0, \quad \xi = 1,$$

$$X(\tau,1) = (\beta + 1)X_1 - \beta\left(\int_0^\tau \frac{\partial X(\tau,0)}{\partial \xi}\ \tau + \int_0^1 X d\xi\right) \tag{A-8}$$

where $\alpha = \pi R^2 L V_1^{-1}$ and $\beta = \pi R^2 L V_2^{-1}$.

Equation (A-5), with the accompanying boundary conditions (A-6), (A-7), and (A-8), is transformed with respect to the independent variable τ, thus letting

$$L[X(\tau,\xi)] = X(s,\xi),$$

and using Eq. (A-6), Eq. (A-5) becomes

$$sX(s,\xi) - X_1 = \frac{d^2X(s,\xi)}{d\xi^2} \quad . \tag{A-9}$$

Solving this ordinary second order differential equation, it is found that

$$X(s,\xi) = A\ (s)\ \sinh\ (\lambda\xi) + B\ (s)\ \cosh\ (\lambda\xi) + \frac{X_1}{s} \tag{A-10}$$

where $\lambda = s^{1/2}$.

To determine the coefficient functions A (s) and B (s) it is observed that the Laplace transforms of boundary conditions (A-7) and (A-8) are

$$\tau > 0, \quad \xi = 0, \quad X(s,0) = s^{-1} + \alpha s^{-1} \frac{dX(s,0)}{d\xi} \tag{A-11}$$

and

$$\tau > 0, \quad \xi = 1, \quad X(s,1) = (\beta + 1)X_1 s^{-1} - \beta s^{-1} \frac{dX(s,0)}{d\xi} - \beta \int_0^1 X(s,\xi)\, d\xi \ . \tag{A-12}$$

Taking the derivative of Eq. (A-10) and applying boundary condition (A-11),

$$B(s) = s^{-1}(1 - X_1) + \alpha s^{-1} \frac{dX(s,0)}{d\xi} \tag{A-13}$$

$$= s^{-1}(1 - X_1) + \alpha s^{-1}[A(s)\, \lambda \cosh(0) + B(s) \sinh(0)]$$

thus

$$B(s) = (1 - X_1)s^{-1} + \alpha A(s)\, \lambda^{-1}. \tag{A-13a}$$

Applying boundary condition (A-12) to Eq. (A-10)

$$A(s) \sinh(\lambda 1) + [(1 - X_1)s^{-1} + \alpha A(s)\, \lambda^{-1}] \cosh(\lambda 1) + X_1 s^{-1} = (\beta + 1)X_1 s^{-1} - \beta A(s)\, \lambda^{-1} - \beta \int_0^1 \{A(s) \sinh(\lambda\xi) + [(1 - X_1)s^{-1} + \alpha A(s)\, \lambda^{-1}] \cosh(\lambda\xi) + X_1 s^{-1}\} d\xi. \tag{A-14}$$

After performing the indicated integration and simplification of Eq. (A-14), the coefficient function A (s) is found to have the form

$$A(s) = (X_1 - 1)[\beta \sinh(\lambda) + \lambda \cosh(\lambda)][(s + \alpha\beta)\lambda \sinh(\lambda) + (\alpha + \beta)s \cosh(\lambda)]^{-1}. \quad \text{(A-15)}$$

Substituting the expressions for A (s) and B (s) into Eq. (A-10) and simplifying gives the solution for $X(s,\xi)$ as a function of the variables s and ξ as follows:

$$X(s,\xi) = X_1 s^{-1} + (1 - X_1)s^{-1} \cosh(\lambda\xi) + (X_1 - 1)s^{-1}[\beta \sinh(\lambda) + \lambda \cosh(\lambda)][\lambda \sinh(\lambda\xi) + \alpha \cosh(\lambda\xi)] \cdot [(s + \alpha\beta) \sinh(\lambda) + (\alpha + \beta)\lambda \cosh(\lambda)]^{-1} \quad \text{(A-16)}$$

In order to use one of Heaviside's expansion theorems in finding the inverse of Eq. (A-16), it is necessary to find the unrepeated roots of both the first and second terms of the equation. Clearly, zero is a root of both terms and only the second term has non-zero roots of higher order. These roots are found by equating the denominator of the second term to zero as follows:

$$s[(\alpha\beta + s) \sinh \lambda + (\alpha + \beta)\lambda \cosh \lambda] = 0 \quad \text{(A-17)}$$

which leads to the expression

$$\tanh \lambda_n = -\lambda_n(\alpha + \beta)/(\alpha\beta + \lambda_n^2). \quad \text{(A-18)}$$

Equation (A-18) has an infinite number of imaginary roots designated by λ_n.

Finding the inverse of Eq. (A-16) by Heaviside's formula using the roots given above yields

$$X(\tau,\xi) = L^{-1}[{}^{1^{st}\ \text{term}}_{\text{zero root}}] + L^{-1}[{}^{2^{nd}\ \text{term}}_{\text{zero root}}]$$

$$+ L^{-1}[{}^{3^{rd}\ \text{term}}_{\text{zero root}}] + L^{-1}[{}^{3^{rd}\ \text{term}}_{\text{negative roots}}] \qquad \text{(A-19)}$$

where

$$L^{-1}[{}^{1^{st}\ \text{term}}_{\text{zero root}}] = X_1 \qquad \text{(A-20)}$$

$$L^{-1}[{}^{2^{nd}\ \text{term}}_{\text{zero root}}] = 1 - X_1 \qquad \text{(A-21)}$$

$$L^{-1}[{}^{3^{rd}\ \text{term}}_{\text{zero root}}] = \theta/\phi\Big|_{\lambda^2 = 0} \qquad \text{(A-22)}$$

where

$$\theta = (X_1 - 1)[\beta \sinh(\lambda) + \lambda \cosh(\lambda)]$$

$$\cdot [\lambda \sinh(\lambda\xi) + \alpha \cosh(\lambda\xi)]e^{\lambda^2\tau}$$

$$\phi = (\alpha\beta + \lambda^2) \sinh(\lambda) + \lambda(\alpha + \beta) \cosh(\lambda) + \lambda^2$$

$$\cdot [(2\lambda)^{-1}(\alpha\beta + \lambda^2 + \alpha + \beta) \cosh(\lambda)$$

$$+ (1/2(\alpha + \beta) + 1) \sinh(\lambda)] \qquad \text{(A-23)}$$

so that

$$\theta/\phi\Big|_{\lambda^2=0} = \alpha(X_1 - 1)(\beta + 1)(\alpha + \beta + \alpha\beta)^{-1}$$

$$L^{-1}[{}^{3^{rd}\ \text{term}}_{\text{negative roots}}] = (X_1 - 1)\sum_{n=1}^{\infty} \theta_n^*/\phi_n^* \qquad \text{(A-24)}$$

where

$$\theta_n^* = [\beta \sinh(\lambda_n) + \lambda_n \cosh(\lambda_n)]$$

$$\cdot [\lambda_n \sinh(\lambda_n \xi) + \alpha \cosh(\lambda_n \xi)] e^{\lambda_n^2 \tau},$$

$$\phi_n^* = \lambda_n^2 [(2\lambda_n)^{-1}(\alpha + \beta + \alpha\beta + \lambda_n^2) \cosh(\lambda_n)$$

$$+ (1/2(\alpha + \beta) + 1) \sinh(\lambda_n)]$$

Equation (A-24) is simplified by redefining λ_n^2 to have a positive value. This operation requires the substitution of $-\lambda_n^2$ for λ_n^2 in Eqs. (A-18) and (A-24). Using the identities

$$\tanh ix = i \tan x,$$

$$\cosh ix = \cos x,$$

$$\sinh ix = i \sin x,$$

and the definition for λ_n^2, causing λ_n to equal $i\lambda_n$, Eqs. (A-18) and (A-24) reduce to

$$\tan \lambda_n = -\lambda_n(\alpha + \beta)/(\alpha\beta - \lambda_n^2) \tag{A-25}$$

and

$$L^{-1}[{}^{3^{rd}\ \text{term}}_{\text{negative roots}}] = -\sum_{n=1}^{\infty} \theta_n^\dagger(\lambda_n, \xi, \tau)/\phi_n^\dagger(\lambda_n) \tag{A-26}$$

where

$$\theta_n^\dagger(\lambda_n, \xi, \tau) = e^{-\lambda_n^2 \tau} [\alpha \cos(\lambda_n \xi) - \lambda_n \sin(\lambda_n \xi)]$$

$$\cdot [\lambda_n \cos \lambda_n + \beta \sin \lambda_n]$$

$$\phi_n^{\dagger}(\lambda_n) = \lambda_n^2((2\lambda_n)^{-1}(\alpha + \beta + \alpha\beta - \lambda_n^2) \cos \lambda_n$$

$$- [1/2(\alpha + \beta) + 1] \sin \beta_n\}.$$

The eigenvalues λ_n of Eq. (A-25) are solved accurately by Newton's method (33) given a close approximation to the actual λ_n values. The first order solution λ_1 is given by

$$\tan \lambda_1 \simeq \lambda_1 = \lambda_1(\alpha + \beta)/(\lambda_1^2 - \alpha\beta) \qquad \text{(A-27)}$$

so that $\lambda_1 \simeq (\alpha + \beta + \alpha\beta)^{1/2}$.
Approximations to higher order values of λ_n are obtained by use of the algorithm $\lambda_n \simeq \lambda_{n-1} + \pi$.

Thus the solution to the partial differential equation (A-5), given by Eq. (A-19), can be written

$$X(\tau,\xi) = (\beta + \alpha X_1[\beta + 1)/(\alpha + \beta + \alpha\beta)$$

$$+ (X_1 - 1) \sum_{n=1}^{\infty} \phi_n^{\dagger}(\lambda_n,\xi,\tau)/\phi_n^{\dagger}(\lambda_n) \qquad \text{(A-28)}$$

where λ_n^2 is a solution to the transcendental equation (A-25). Equation (A-27) shows the change in concentration gradient at a distance variable point z with respect to time as a function of the system parameters V_1, V_2, R, L, and D.

7.2 APPENDIX B

Leakage Error Analysis

In order to correct for leakage of the tracer gas prior to opening of the capillary valve, "10", Mistler subtracted a "background" value from all experimental count rates in each run. This subtraction forced the normalized count rates to fit the boundary conditions of his mathematical model. The model assumed zero concentration of the tracer gas in the capillary tube and right-hand flask at the time of opening of the capillary valve. The "background" count rate, k_1, was obtained by solving the equation

$$(C_\infty - k_1)(C_o - k_1)^{-1} = \beta(\alpha + \beta + \alpha\beta)^{-1} \qquad \text{(B-1)}$$

where C_∞ = the observed equilibrium count rate,

C_o = the observed initial count rate,

α and β are defined as in Appendix A,

$\beta(\alpha+\beta+\alpha\beta)^{-1}$ = the normalized equilibrium concentration for an initial zero concentration of tracer gas in the tube and right-hand flask.

If a quantity X_∞^C is defined as

$$X_\infty^C \equiv \beta(\alpha+\beta+\alpha\beta)^{-1} \qquad \text{(B-2)}$$

the solution of Eq. (B-1) for k_1 yields

$$k_1 = (C_\infty - C_o X_\infty^C)(1 - X_\infty^C)^{-1} \qquad \text{(B-3)}$$

If it is noted that in most circumstances only the first term of the summation makes a significant contribution, an approximate diffusion coefficient is found to be

$$D' = -L^2(\lambda_1^2 t_i)^{-1} \ln(-(X_{ia}-X_\infty^c)A_1^{-1} \quad . \tag{B-7}$$

If in the solution as found in Appendix A the same approximation of utilizing only the first term of the series is applied, the diffusion coefficient becomes

$$D = -L^2(s_1 t_i)^{-1} \ln(-(X_i-X_\infty)(1-X_\infty^c)(A_1(1-X_\infty))^{-1}) \tag{B-8}$$

Based on these assumptions, the error associated with Mistler's approximation is for the i^{th} observation

$$D - D' = -L^2(s_1 t_i)^{-1} \ln(X_i-X_\infty)(1-X_\infty^c)((1-X_\infty)(X_{ia}-X_\infty^c))^{-1}) \tag{B-9}$$

The computer code ERCALC was used to compute the value of this error. As shown in Appendix A, the normalized count rate, X_i, at time, t_i, is given by

$$X_i = X_\infty + (X_1-1) \sum_{n=1}^{\infty} A_n e^{-\lambda_n^2 \tau_i} \tag{B-10}$$

where X_1 and τ_i are defined as in Appendix A. It is noted that t_i is contained in τ_i as

$$\tau_i = t_i D L^{-2}. \tag{B-11}$$

Performance of the described subtraction gives the approximate value of the i^{th} normalized concentration as

$$X_{ia} = (C_i(1-X_\infty^C) - C_\infty + C_o X_\infty^C)(C_o(1-X_\infty^C) - C_\infty + C_o X_\infty^C)^{-1} \quad . \qquad (B\text{-}4)$$

in terms of concentrations normalized by the observed initial count rate this is

$$X_{ja} = (X_i(1-X_\infty^C) - X_\infty + X_\infty^C)(1-X_\infty)^{-1} \quad , \qquad (B\text{-}5)$$

where X_i is the i^{th} normalized concentration as used in the solution for a finite initial concentration in the capillary tube and right-hand flask (Appendix A).

Mistler's model was

$$X_{ia} = \beta(\alpha+\beta+\alpha\beta)^{-1} - \sum_{n=1}^{\infty} A_n \, e^{-t_i \lambda_n^2 D/L^2} \quad . \qquad (B\text{-}6)$$

where

$$A_n = [\theta_n^\dagger(\lambda_n, \xi, \tau)/\phi_n^\dagger(\lambda_n)]e^{\lambda_n^2 \tau}$$

and

$$\theta_n^\dagger(\lambda_n, \xi, \tau), \phi_n^\dagger(\lambda_n) \quad ,$$

and

λ_n are defined in Appendix A.

Representative values of X_∞ and X_1 were chosen and used as input values to ERCALC. Values of D ranging from 100 to 1000 cm^2/sec were employed as were values of t_i for each value of D. The values of t_i were chosen so as to span the transient time of the system for that D.

The subroutine XCALF was called within ERCALC for each D and its associated t_i's, and by use of Eq. (B-10) values of X_i were generated. ERCALC then computed the error of Mistler's approximation by Eq. (B-9) at each value of t_i for each D.

The maximum magnitude of this error in all cases investigated was found to be considerably less than 1%. This indicated that the error induced by Mistler's approximation was negligible when compared with the other sources of error he encountered.

7.3 APPENDIX C

Data Analysis for the Diffusion Coefficient

7.3.1 Computer Program

A computer program previously developed by Mistler for analysis of data from this system was modified to agree with the solution for the system with an initial concentration of tracer gas in the capillary tube and right hand flask (See Appendix A). Basically, as in its original form, the program performs an iterative least squares analysis to determine the "best" value for the effective diffusion coefficient. Minor additions were made to allow internal normalization of data points and the association of a time with each point. A subroutine was added to the program to calculate the increase of the variance of the experimental diffusion coefficient caused by uncertainty in pressure measurements (See Section 2.6.2). A brief discussion of the least squares analysis follows.

7.3.2 Least Squares Analysis and Numerical Approximations

In the method of least squares (9) the sum of the squares of deviations, Re, between the observed values, Xe_i, and the Xc_i, are minimized to find the values of Xc_i which give the minimum error. Applying this method of analysis to the diffusion data the expression for the residue, Re, is

$$Re = \sum_{i=1}^{N} (Xe_i - Xc_i)^2 \qquad (C\text{-}1)$$

where Xe_i and Xc_i are the i^{th} experimental and calculated values of X at time t_i respectively, and N is the number of data points. The minimum squared error is found by differentiating Re with respect to D and setting the resultant equal to zero; thus,

$$\frac{\partial Re}{\partial D} = -2 \sum_{i=1}^{N} (Xe_i - Xc_i) \frac{\partial Xc_i}{\partial D} = 0 \quad . \qquad (C\text{-}2)$$

Defining a quantity

$$f_D = \sum_{i=1}^{N} (Xe_i - Xc_i) \frac{\partial Xc_i}{\partial D}$$

and utilizing the first two terms of Taylor's expansion (33) the result is

$$f_D = f_{D_o} + \overline{\Delta D} \frac{\partial f_D}{\partial D} \qquad (C\text{-}3)$$

where f_D should be zero by Eq. (C-2) so that

$$\overline{\Delta D} = -f_{D_o} \left[\frac{\partial f_D}{\partial D} \right]^{-1} \quad . \qquad (C\text{-}4)$$

To evaluate the right hand member of Eq. (C-4) use

$$\frac{\partial f_D}{\partial D} = \sum_{i=1}^{N} \left| (Xe_i - Xc_i) \frac{\partial^2 Xc_i}{\partial D^2} - \left(\frac{\partial Xc_i}{\partial D} \right)^2 \right| \qquad (C\text{-}5)$$

where

$$\frac{\partial Xc_i}{\partial D} = \sum_{i=1}^{N} (\lambda_n^2 \tau / L^2)\, \theta_n^{\dagger}(\lambda_n, \xi, \tau) / \phi_n^{\dagger}(\lambda_n) \qquad \text{(C-6)}$$

$$\frac{\partial^2 Xc_i}{\partial D^2} = - \sum_{i=1}^{N} (\lambda_n^2 \tau / L^2)^2\, \theta_n^{\dagger}(\lambda_n, \xi, \tau) / \phi_n^{\dagger}(\lambda_n) \ . \qquad \text{(C-7)}$$

where λ_n, τ, L, ξ, $\theta_n^{\dagger}$, and $\phi_n^{\dagger}$ are defined as in Appendix A. The value of D with minimum error can be determined by using the algorithm $D_{n+1} = D_n + \overline{\Delta D}$ and iterating upon D until $\overline{\Delta D}$ is sufficiently small.

7.4 APPENDIX D

Experimental Procedure

Prior to the actual accumulation of data, several preparations were necessary. After carefully installing the surface barrier detector, all valves except "15", Fig. (5), were left open with the vacuum pump running for approximately 24 hours. This allowed complete desorption of water vapor adsorbed on the glass surfaces of the system during exposure to the atmosphere and attainment of a pressure of approximately 1μ of Hg. After degassing, the rate of desorption was so slow that there was no detectable pressure change during the time required for an experiment. This time ranged from 20 to 60 minutes approximately.

The system was then purged with CH_4 or CO_2 a minimum of six times. For each purge, the pressure throughout the system was raised to approximately 500 mm of Hg by closing valve "9" and bleeding the appropriate gas in through valve "15". Valve "15" was then closed, the vacuum pump reintroduced, and the system evacuated to 1μ of Hg.

After purging, valves "2", "3", and "4" were closed and the radioactive gas flask removed. The glass stem of the ampoule was broken with a short glass rod housed in the charging flask and the flask replaced. Valves "3", and "4" were opened and the system again thoroughly purged.

To calibrate the thermocouple vacuum gauges, the pressure was again raised to approximately 500 mm of Hg by introducing CH_4 or CO_2, and the system evacuated to the upper portion of the pressure range of interest, approximately 500μ of Hg. After a period of approximately three minutes (valve "11", "5" and "12" remained open throughout the calibration to afford rapid pressure equalization) to allow establishment of pressure equilibrium throughout the system, pressure readings were recorded from the electrical vacuum gauges, "6" and "18", and from the McLeod vacuum gauge. The pressure of the system was lowered a few microns of Hg and after approximately three minutes the gauge readings were recorded. These steps were repeated until the pressure was approximately one micron of Hg. The pressure was again raised to approximately 500 mm of Hg and another traverse of the pressure range made. This procedure was continued until enough readings had been amassed to construct reliable calibration curves for the thermocouple vacuum gauges.

The integrity of the vacuum was checked daily and occasional spot checks were made of the calibration curves. The thermocouple gauges showed no drift from day to day, but the reproducibility of the readings varied somewhat during alternate charging and evacuation of the system.

In order to guard against drift in the electronic equipment, all components except the oscilloscope were supplied power by a Beckman line voltage regulator. Ground loops were prevented by connecting all plug ground lines to receptacle grounds and by

connecting all chassis to a common ground. To prevent the detection of ambient electromagnetic noise signals flask I was enclosed in a wire mesh which was electrically grounded.

To determine usable settings for the electronic equipment, valves "11" and "9" were closed and flask I charged to a pressure of approximately 75μ of Hg with radioactive gas. With arbitrary settings of the amplifier gain and postamplifier gain and a low postamplifier bias setting the output signal was monitored with the oscilloscope. The detector bias voltage was then raised in small increments and the amount of noise in the output signal observed on the oscilloscope. After an initial increase, the noise level decreased to a minimum at an indicated detector bias of 100 volts. Combinations of settings for the amplifier, postamplifier, and multiscaler gains and the postamplifier bias were investigated. Settings of x8 for the amplifier gain, x4 for the postamplifier gain, x3.0 for the multiscaler, and 1.10 for the postamplifier were selected on the basis of maximum count rate with minimum noise. The frequency of the square wave generator signal was calibrated with a stop watch.

The actual diffusion data was taken by the following steps:

1. A time increment for the square wave generator suitable for the desired pressure was chosen and set on the generator by stopwatch.
2. The water level in the constant temperature bath was lowered below the level of the capillary valve. The flap in the wire screen shield was opened and the tape

on the flask removed. The capillary valve, "10", was then closed and visibly inspected. The tape was replaced, the screen flap closed, and the bath refilled.

3. The system was evacuated to a pressure of approximately 1μ of Hg and valve "9" closed.
4. Valve "15" was used to bleed CH_4 or CO_2 into the system and raise the pressure to a level approximately 75μ of Hg less than that desired for the experiment.
5. Valves "11" and "12" were closed, and gas bled into II until its pressure reached that desired for the determination.
6. Valves "2" and "4" were opened and radioactive gas bled into flask I through needle valve "3" to bring it to the desired pressure. Valves "2", "3", and "4" were then closed.
7. The detector voltage was raised to 100v. and the oscilloscope turned on.
8. After a period of two to three minutes the readings of gauges "6" and "18" were recorded and "5" and "13" closed.
9. The output signal was monitored on the oscilloscope as a check on the signal quality.
10. The multiscaler was started and at the time it entered channel number 11, the capillary tube valve was opened.
11. After the multiscaler terminated counting, the trace was printed out with the automatic printer.

12. The trace was visibly inspected on the multiscaler for reliability and attainment of equilibrium.
13. If equilibrium was not reached in the initial trace, a second trace was made to record the equilibrium value and printed out.
14. Valves "5" and "13" were opened and after two to three minutes the final pressure readings were recorded.
15. The system was then purged in preparation for the next determination.

7.5 APPENDIX E

Error Associated with Pressure Gradients

Although efforts were made at the start of each experimental determination to insure constant pressure throughout the system, there is reasonable cause to believe that this was not always accomplished. Small differences in the initial and final readings of the pressure gauges occassionally occurred. Even in the absence of these changes in pressure indications, the small scatter in the calibration curves would lead to reasonable doubt of the assumption of constant initial pressure throughout the system in each determination. The presence of an initial pressure difference between the two flasks would cause a transfer of material in addition to that resulting from diffusive flow along the concentration gradient. The direction of this pressure-induced flow may be in the same or opposite direction as the diffusive flow depending upon the relationship of the total pressure gradient and the concentration gradient of the diffusing material. A study of superimposed pressure-induced and diffusive flow in graphite has been presented by Evans, Truitt, and Watson (23); an analysis for a capillary tube is given by Otani, Wakao, and Smith (56). Based on earlier work by Evans, Watson, and Mason (22), Rothfeld (66), and Scott and Dullien (67), they state the total flux of component 1 in a binary system of 1 and 2 in the presence of both a total pressure gradient and a gradient in the partial pressure of 1 as

$$N_1^* = -D_{12} \frac{dC_1}{dz} [1-(1-m)y_1 + D_{12}/D_{K1}]^{-1} + Fy_1[1+ \frac{D_{12}}{D_{K1}}] \quad (E-1)$$

where D_{12} = the mutual diffusion coefficient according to bulk diffusion theory, cm^2/sec.

C_1 = the concentration of 1, g - mole/cm^3

z = distance in direction of diffusion, cm

m = the square root of the ratio of the molecular weight of 1 to that of 2

y_1 = the mole fraction of 1

D_{K1} = the Knudsen diffusion coefficient of 1, cm^2/sec

F = flux caused by a pressure gradient, g-mole/sec-cm^2

The value of F is given to be

$$F = -[r^2P/8\mu+4rRT/(3(M_1\bar{v}_1y_1+M_2\bar{v}_2y_2))](1/RT) \frac{dP}{dz} \quad (E-2)$$

where r = radius of the capillary tube, cm

P = total average pressure, dynes/cm^2

μ = gas viscosity, poises

R = gas constant, ergs/g-mole-°K

T = temperature, °K

M_1M_2 = molecular weights of 1 and 2, respectively, gm/g-mole

$\bar{v}_1;\bar{v}_2$ = mean molecular speeds of 1 and 2, cm/sec

y_2 = mole fraction of 2.

In the case of isotopic self-diffusion m is approximately unity and Eq. (E-1) reduces approximately to

$$N_1^* = -D_{ell} \frac{dC_1}{dz} + (D_{ell}/D_{11})F\, y_1 \quad (E-3)$$

where D_{e11} = effective diffusion coefficient according to Bosanquet, cm^2/sec

D_{11} = self diffusion coefficient according to bulk diffusion theory, cm^2/sec

1 = subscript denoting tracer gas.

Under these conditions F becomes

$$F = -(r^2P/8\mu+4rRT/3M\bar{v})(1/RT)(\Delta P/L) \qquad (E-4)$$

where L = capillary tube length, cm.

The assumption of a linear pressure gradient in the tube allows replacement of $\frac{dP}{dz}$ by $\Delta P/L$ where ΔP is the pressure difference of the two flasks in the system used in this study ($\Delta P > 0$ when the pressure in flask I is the greater).

By the definition of F and ΔP it may be stated that

$$\frac{d(\Delta P)}{dt} = (D_{e11}/D_{11})ART(1/V_1+1/V_2)F \qquad (E-5)$$

where A = cross sectional area of capillary tube, cm^2

and V_1, V_2 refer to the volumes of the flasks.

By combining Eqs. (E-4) and (E-5)

$$\frac{d(\Delta P)}{dt} = -k_1\Delta P \qquad (E-6)$$

where $k_1 = (D_{e11}/D_{11})(rP/8\mu+4rRT/3M\bar{v})(A/L)(1/V_1+1/V_2)$. The solution of Eq. (E-6) with appropriate boundary conditions gives

$$\Delta P(t) = \Delta P_o\, e^{-k_1 t} \qquad (E-7)$$

In terms of an effective half-life then

$$T_{1/2} = 0.693/k_1 \quad . \tag{E-7A}$$

The quantity $T_{1/2}$ is by definition the time required for an initial pressure difference to decrease to one half its original value. Experimental evaluation of $T_{1/2}$ by the above equations shows that it ranges in value from approximately 330 sec. at a pressure of 50μ to approximately 70 sec. at 500μ.

The observed change in the concentration of tagged material in flask I is directly proportional to the change in the normalized count rate which may be represented as

$$\Delta X_T = \Delta X_d + \Delta X_F \tag{E-8}$$

where ΔX_T = the total observed change in normalized count rate.

ΔX_d = the contribution of diffusion to this change

ΔX_F = the contribution of pressure-induced flow.

The evaluation of these quantities requires the manipulation of Eq. (E-3) to extract expressions for diffusive and pressure-induced flow as functions of time. To avoid this procedure which is quite complicated and of an iterative nature, it was assumed that

$$\Delta X_F = k_2 N^*_{oF} e^{-k_1 t} \tag{E-9}$$

where k_2 is a proportionality constant and Eq. (E-7) was implied. Here N^*_{oF} is the initial flux of tagged material leaving flask I because of the pressure gradient.

If it is assumed that for a short period of time the contributions of diffusive and pressure-induced flow are of the same relative importance as at time zero

$$\left.\frac{\Delta Xd}{\Delta XF}\right|_{t=0} = \frac{N^*_{od}}{N^*_{oF}} \qquad \text{(E-10)}$$

where N^*_{od} is the initial flux of tagged material leaving flask I by diffusive flow. Knowledge of the initial concentrations of tracer in the flasks, the assumption of a constant concentration gradient along the length of the tube, and an estimate of $D_{e_{11}}$ allows the evaluation of N^*_{od} by

$$N^*_{od} = -D_{e_{11}} \left.\frac{dC_1}{dx}\right|_{t=0} \qquad \text{(E-11)}$$

If the pressure and ΔP_o are also known N^*_{oF} is obtained from

$$N^*_{oF} = (D_{e_{11}}/D_{11})\ F\ y_1\ |_{t=0} \quad . \qquad \text{(E-12)}$$

By use of the system solution with the estimate of $D_{e_{11}}$ as given in Appendix A the value of ΔX_d may be found when $t = \Delta t$ and Eq. (E-10) may be solved for the value of ΔX_F. Substitution of ΔX_F and Δt into Eq. (E-9) allows solution for k_2. All the quantities necessary to evaluate ΔX_F by Eq. (E-9) are then known, and the effect of pressure-induced flow may be removed from data by continued use of Eq. (E-9) and

$$\Delta X_d = \Delta X_T - \Delta X_F \qquad \text{(E-13)}$$

where ΔX_T is the observed change in the normalized count rate at time t.

The significance of this correction was investigated by applying it to representative sets of data which had already been analyzed. A computer code was written to do this and sets of data covering the pressure range analyzed. An estimate of ΔP_o was determined from the initial readings of the pressure gauges and the gauge calibration curves and an estimate of D_{e11} from the original least squares analysis. The original data was corrected by use of Eq. (E-13) and again subjected to the least squares analysis. In all the cases investigated, the corrected diffusion coefficient differed from that obtained from the uncorrected data by less than 1%. For the sample data set presented in Table I, this correction increased the resultant D_{e11} from 614.3 to 617.4 cm^2/sec an increase of approximately 0.5%.

ISOTOPIC GASEOUS SELF-DIFFUSION COEFFICIENTS AT TRANSITIONAL PRESSURES

by

GLEN ROY CORRELL

B. S., University of Missouri at Rolla, 1965

AN ABSTRACT OF A MASTER'S THESIS

submitted in partial fulfillment of the

requirements for the degree

MASTER OF SCIENCE

Department of Nuclear Engineering

KANSAS STATE UNIVERSITY
Manhattan, Kansas

1967

ABSTRACT

A modified Ney-Armistead diffusion cell utilizing a semiconductor radiation detector was used to measure self-diffusion coefficients of CO_2 and CH_4 at 20°C in the transition pressure range. Summaries of existing theories of gaseous diffusion in the bulk, Knudsen, and transition region were presented. The existing methods of diffusion coefficient measurement were summarized. The properties, characteristics, and advantages of semiconductor radiation detectors were discussed. Descriptions of the experimental arrangements and techniques and the methods of data analysis were given detailed treatment. The significance of results was discussed and an extensive error analysis presented.

The diffusion cell consisted of two flasks of 579 ml and 512 ml joined by a capillary tube 10.00 cm long and 0.126 cm I.D. A surface-barrier radiation detector was contained within the large flask. The effective tube length was determined by use of the Rayleigh end-correction.[1] A solution of the one-dimensional diffusion partial differential equation was obtained by the application of Fick's second law and the use of Laplace transforms. Data consisting of concentration versus time was subjected to an iterative least squares analysis to determine the effective diffusion coefficient.

The semiconductor radiation detector was found to have the advantages of internal detection of radioactive tracers, rapid time response, and high counting efficiency. Refinements of the

apparatus and analysis were employed to reduce the errors encountered by Mistler[2] and to increase the value of this approach for measurement of effective diffusion coefficients in the transition pressure range.

Values of the self-diffusion coefficient of CO_2 were presented which supported Mistler's findings. Effective diffusion coefficients were reported for CH_4 over a pressure range of 50 to 500 microns. Those between 50 and 300 microns agreed within 10% with the theory of Bosanquet while those from 300 to 500 microns exceeded predicted values by as much as 12.3%. Errors were attributed primarily to surface diffusion effects not considered in the analysis. Standard deviations based on the residues of the least squares analysis and uncertainties of pressure measurement were generally 2-3%, with isolated values as high as 5.5% near 50 microns.

---

[1] Rayleigh, Lord, Theory of Sound. Dover Publications, 2, 291 (New York, 1945.

[2] Mistler, T. E., Radioactive Tracer Determinations of Gaseous Diffusion Coefficients. M.S. Thesis, Kansas State University, Manhattan, Kansas, 1966.